PNNL-11965

Pacific Northwest National Laboratory
Operated by Battelle for the U.S. Department of Energy

Effects of Aging Quartz Sand and Hanford Site Sediment with Sodium Hydroxide on Radionuclide Sorption Coefficients and Sediment Physical and Hydrologic Properties: Final Report for Subtask 2a

D. I. Kaplan
K. E. Parker
J. C. Ritter

October 1998

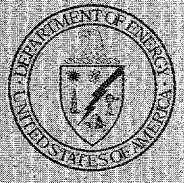

Prepared for the U.S. Department of Energy
under Contract DE-AC06-76RLO 1830

DISCLAIMER

PACIFIC NORTHWEST NATIONAL LABORATORY
operated by
BATTELLE
for the
UNITED STATES DEPARTMENT OF ENERGY
under Contract DE-AC06-76RLO 1830

Printed in the United States of America

Available to DOE and DOE contractors from the Office of Scientific and Technical Information, P.O. Box 62, Oak Ridge, TN 37831; prices available from (615) 576-8401.

Available to the public from the National Technical Information Service, U.S. Department of Commerce, 5285 Port Royal Rd., Springfield, VA 22161

PNNL-11965

Effects of Aging Quartz Sand and Hanford Site Sediment with Sodium Hydroxide on Radionuclide Sorption Coefficients and Sediment Physical and Hydrologic Properties: Final Report for Subtask 2a

D. I. Kaplan
K. E. Parker
J. C. Ritter

October 1998

Prepared for
the U.S. Department of Energy
under Contract DE-AC06-76RLO 1830

Pacific Northwest National Laboratory
Richland, Washington 99352

Summary

Column and batch experiments were conducted in fiscal year 1998 at Pacific Northwest National Laboratory[1] to evaluate the effect of varying concentrations of NaOH on the sorptive, physical, and hydraulic properties of two media: a quartz sand and a composite subsurface sediment from the 200-East Area of the Hanford Site. The NaOH solutions were used as a simplified effluent from a low-activity glass waste form. These experiments were conducted over a limited (0- to 10-month) contact time, with respect to the 10,000- to 100,000-year scenarios described in the Immobilized Low-Activity Waste-Performance Assessment (ILAW-PA).

When these two solids were put in contact with the NaOH solutions, dissolution was evident by a substantial increase in dissolved Si concentrations in the leachates. Incremental increases in NaOH concentrations, resulted in corresponding increases in Si concentrations. A number of physical and hydraulic properties also changed as the NaOH concentrations were changed.

It was observed that quartz sand was less reactive than the composite sediment. Further, moisture-retention measurements were made on the quartz sand and composite sediment, which showed that the NaOH-treated solids retained more water than the non-NaOH-treated solids. Because the other chemical, physical, and hydraulic measurements did not change dramatically after the high-NaOH treatments, the greater moisture retention of the high-NaOH treatments was attributed to a "salt effect" and not to the formation of small particles during the dissolution (weathering).

The distribution coefficients (K_ds) for Cs and Sr were measured on the NaOH-treated sediments, with decreases from ~3,000 to 1,000 and 1,300 to 300 mL/g noted, respectively, at the 0.01- to 1.0-M NaOH levels. There was no apparent trend for the Sr K_d values with contact time. The lack of such a trend suggests that dissolution of sediment particles is not controlling the drop in K_d; rather, it is the competition of the added Na in the various treatment solutions.

It is clear from these experiments that the background chemistry of the waste-glass leachate is likely to have a significant effect on the hydrology and radionuclide geochemistry in the near-field environment of the ILAW. These experiments provided an important first approximation of several chemical and physical processes. Future research, together with the data presented in this report, will provide important guidance for the selection of near-field hydraulic and geochemical input data for the ILAW-PA.

[1] Pacific Northwest National Laboratory is operated by Battelle for the U.S. Department of Energy.

Contents

Figures

Tables

1.0 Introduction

The leachate from the glass waste forms and the cement encasement that may be used at the Immobilized Low-Activity Waste-Disposal Complex (ILAW-DC) will have very high pH and ionic strength (Mann et al. 1998). High-ionic-strength and pH effluent may alter the sorptive tendencies of the sediment hydrology, physics, mineralogy, and radionuclides. For example, it is known that such solutions may dissolve silicate or aluminosilicate minerals (Dress et al. 1989), and the presence of such high-salt concentrations may increase competition for sorption sites on mineral surfaces (Sposito 1989, Kaplan et al. 1998a) and increase the moisture retention of sediments (Hillel 1980). One concern for the ILAW-Performance Assessment (-PA) is that the sorptive and hydraulic properties of the near-field materials will change once the plume emanating from the waste form enters this region. Among the near-field materials that the plume may come into contact with are a backfill material and a capillary-break barrier material. Should dissolution of these materials occur, the distribution coefficients (K_ds) for radionuclides, particle-size distribution, porosity, bulk density, moisture retention, and hydraulic conductivity would be expected to change. This lack of knowledge could adversely affect the ILAW-PA by increasing uncertainty and requiring unrealistically conservative estimates as input parameters.

There have not been any long-term studies conducted to evaluate the effect of high-ionic-strength and high-pH conditions on Hanford Site sediment physical, hydrologic, and sorptive properties. Previous experiments looked primarily at the rather short-term (30-day) effects of high salt and high pH on radionuclide sorption. Those experiments were not designed to evaluate such important effects as dissolution of the sediment in the presence of such solutions.

1.1 Objectives

The objectives of this study were to evaluate the effects of high pH and high ionic strength on the hydraulic, physical, and sorptive properties of a quartz sand and a Hanford Site sediment collected from the subsurface of the 200-East Area. Attention was directed at trying to separate "salt effects" from "dissolution effects" through the measurement of a number of bulk sediment properties.

1.2 Scope

The scope of this study was to conduct a series of batch and column experiments to evaluate the effects of simulated glass leachates on Cs, Sr, and U K_d values and sediment physical and hydrologic properties. A partial factorial experimental design was conducted with the following variables: type of experiment (batch or column), NaOH concentration (0, 0.01, 0.1, and 1.0 M), contact time (0, 1, 2, and 10 months), and 3 replications. The 0-M NaOH is equivalent to deionized water. A number of physical, hydrologic, and geochemical parameters were measured, including moisture-retention curve data, particle-size distribution, hydraulic conductivity, porosity, bulk density, and aqueous cation concentration. NaOH

was selected as the surrogate for glass leachate because it consists of the two dominant ions expected to exist in the actual glass leachate (Mann et al. 1998).

The Hanford Site composite sediment selected for these studies is representative of material that may be used in the near field of the ILAW-DC as backfill material. The coarse-textured sand was selected for these experiments to provide information relevant to the capillary-break material that may be used in the engineered barrier around the immobilized glass waste. Preliminary modeling of the near field indicated that diffusion may cause some of the glass leachate to migrate upward toward the capillary-break barrier (Mann et al. 1998). It was expected that the sand would provide a worst-case scenario because it has a finer texture and, therefore, a greater surface-to-volume ratio for reactivity to the aqueous phase than the actual material being considered for the barrier.

These experiments, conducted at the Pacific Northwest National Laboratory will be continued into fiscal year 1999. This additional research will apply more direct measurements using an x-ray tomography unit, and will be conducted using more complex, simulated glass leachates than were used in the studies presented here. Particular attention will be directed at quantifying the reaction rates of mineral dissolution and defining the solid-phase composition of a Hanford Site backfill sediment after extended exposure to the synthetic glass leachate. The intent of this and future research is to provide guidance for the selection of near-field hydraulic and geochemical input data for the ILAW-PA.

1.3 Background

As part of the ILAW-PA, the effects of ionic strength and pH on U(VI) sorption were evaluated through a series of batch-type laboratory experiments (Kaplan et al. 1996, 1998b). U(VI) K_d and solubility values did not change as the ionic strength was increased with $NaClO_4$ to 0.014 M. U(VI) K_d values essentially doubled from 1.07 to 2.22 mL/g as the pH of the system increased from 8.3 to 9.3. Above pH 10.3, precipitation of U(VI)-containing solids occurred, resulting in apparent K_d values of >400 mL/g. Precipitation did not occur in tubes with pH-adjusted solution only. Sediment had to be present to effect U(VI) precipitation. This suggests that heterogeneous precipitation occurred (i.e., foreign "seed crystals" [the sediment] were necessary). Thus, in carbonate systems with a pH greater than ~10.5, U(VI) mobility may be much less than in near-neutral pH systems. These results have significant ramifications for the ILAW-PA, in that in areas where high-pH levels are expected (e.g., near the glass waste), quite high K_d values for U(VI) can be justified.

K_d values of Se and Tc have also been observed to increase as ionic strength increases (Kaplan et al. 1998c). In the case of Se, the K_d values increase from 3.31 ± 0.57 to 4.11 ± 0.06 mL/g as the solution ionic strength increases from ~50 to 500 mM. Over the same increase in ionic strength, Tc K_d values increased from 0.16 ± 0.04 to 3.94 ± 0.99 mL/g. The cause for this increase in K_d values is likely that the higher ionic strength caused the double layer around the particles to decrease, thereby permitting greater TcO_4^- and I^- interaction with the mineral surfaces. The closer contact of the TcO_4^- with the mineral surface enhanced contact between the anion and the positively charged sorption sites. Hanford Site sediments have few positively charged sorption sites at the alkaline pH that these studies were conducted (pH

~8). However, these few sites may play an important role, especially at the extremely low Se and Tc concentrations (in the nanomole range) used in these experiments and expected in portions of the ILAW-DC.

Pore-water pH also had a significant effect on the sorption of Tc (added as TcO_4^-), Se (added as SeO_4^{2-}), and I (added as I^-) (Kaplan et al. 1998c). As the pH increased from 8.1 (natural Hanford Site background) to 11.9, I K_d values decreased from 0.22 ± 0.01 to 0.01 ± 0.01 mL/g and Se K_d values decreased from 5.78 ± 0.28 to 0.04 ± 0.00 mL/g. This pH K_d trend is consistent with the general rule that anion sorption decreases as the pH increases because increases in pH tend to increase the negative surface charge of minerals. This trend was not observed for Tc K_d values. Instead, as the pH increased from 8.1 to 11.9, the Tc K_d values increased from -0.02 ± 0.01 to 1.07 ± 0.03 mL/g. The cause for this unexpected but very consistent trend is not known. One possible explanation is that the modest increase in ionic strength that concomitantly increased with pH increases may have been responsible for the enhanced removal of TcO_4^- from the aqueous phase. Precipitation is an unlikely removal mechanism; neither thermodynamic solubility calculations nor aqueous-phase filtration of pH 11.9 TcO_4^- solutions suggested the formation of precipitated Tc phases.

As mentioned, the waste-glass leachate may also have a significant effect on the sediment's physical state and hydrology. These effects can be broadly categorized as "dissolution effects" and "salt effects." The dissolution effects are rather obvious (i.e., as the individual particles dissolved, the porosity increased, bulk density decreased, and hydraulic conductivity increased). If the dissolved constituents reprecipitate, these trends may, in fact, reverse. The reprecipitated particles would tend to be small and may plug the porous media. The "salt effect" impacts the physical properties of the water (i.e., colligative properties [e.g., freezing point, boiling point, vapor pressure], density, osmotic potential, dielectric constant, and surface tension).

The propensity of a sediment to hold onto soil moisture under unsaturated conditions is largely controlled by its matrix potential (Hillel 1980). Pneumatic potential may also be important, but this effect is negligible in laboratory studies where the atmospheric pressure remains nearly constant, small barometric pressure fluctuations notwithstanding. Matrix potential is related to two processes, water adsorption to the sediment surface and capillary forces. The adsorption of water onto mineral surfaces is influenced by the electric double layer and the exchangeable cations present. Water adsorption is an exothermic process, resulting in the liberation of an amount of heat known as the heat of wetting. Anderson (1926, as cited in Hillel 1980) found a linear relationship between heat of wetting and cation-exchange capacity. Presumably, this relationship is the result of adsorbed cations having water molecules associated with them (water of hydration). Therefore, as more hydrated cations adsorb to a sediment's surfaces, the more water molecules will be associated with the mineral surfaces. Janert (1934, as cited in Hillel 1980) reported a relationship between the heat of wetting and the nature of the cation on the exchange site. Generally, the greater the charge density of the ion (i.e., the ratio of charge to surface area of the ion), the more heavily hydrated the ion will be. Another general rule is that anions exhibit less hydration than cations. This is because it is energetically easier for water molecules to orient themselves with the protons outward and the negative end inward toward the positively charged cation at the center of the hydrated cluster. A typical Coulombic (electrostatic) hydration envelope around a cation consists of an inner sphere of strongly bound molecules surrounded by an outer shell of less strongly bound water

molecules. A surface hydrated with monovalent cation at 10°C may have adsorbed water molecules that reach out 1 to 6 nm into the bulk water, which is ~3 to 18 water molecules thick.

In addition to water adsorption, capillary forces influence matrix potential. Capillary forces increase with decreased pore size (or decreased particle size) and increased surface tension.

$$h_c = (2\gamma \cos\alpha)/g(\rho_l - \rho_g)r \quad (1)$$

where h_c is the capillary height above free water; γ is the surface tension between the liquid and the air; α is the contact angle between the water and the solid phase; g is the acceleration of gravity; ρ_l and ρ_g are the density of the liquid and the gas, respectively; and r is the capillary radius. The presence of dissolved electrolytes decreases the potential energy of water that, in turn, increases the surface tension of water. Surface tension is a phenomenon occurring typically at the interface of a liquid and a gas. If the affinity of the solute molecules (ions) to water molecules is greater than the affinity of the water molecules to one another, then the solute tends to be drawn into the solution that causes an increase in the surface tension. Electrolytes tend to have a greater affinity for water molecules than water molecules have to each other. The important point to note from this discussion is that salts can increase surface tension, and from Equation (1), it becomes apparent that surface tension affects capillary forces (i.e., the greater the surface tension, the greater the capillary forces).

In heterogeneous, unsorted, natural sediments, water adsorption and capillary forces are significant. In sandy soils, water adsorption is relatively unimportant and the capillary effect predominates. The opposite is true in sediments containing more fine-grained particles (i.e., the capillary effect is relatively unimportant and adsorption is more important).

Moisture-retention curves provide information about the amount of moisture retained by an unsaturated soil at given water potential. The data are generated, in part, by placing a soil core on a pressure plate that permits varying degrees of negative pressure (i.e., suction to be applied). In a saturated sediment at equilibrium with free water at the same elevation, the pressure exerted on the water is equal to atmospheric pressure, thus hydrostatic pressure equals atmospheric pressure and water potential is equal to zero bar. If a slight negative water potential is applied (i.e., a water pressure slightly subatmospheric), no water will flow out until a critical suction is exceeded. This critical value is referred to as the air-entry potential. As suction is increased, water is drawn out of the soil and more of the relatively large pores, which cannot retain water against the applied suction, will empty. By assuming that the contact angle is zero and that soil pores are cylindrical, a simple relationship exists between the minimum radius of a pore (r) that will drain at a given applied negative potential (-P, or suction):

$$-P = 2\gamma/r \quad (2)$$

where γ is the aqueous-phase surface tension (pure water = 71.9 g/s^2 at 25°C). Equation (2) shows that as the applied suction is increased for a given solution, smaller pores will be drained. Increasing suction is, therefore, associated with decreasing soil wetness. Perhaps more germane to this discussion is that Equation (2) shows that, as the surface tension increases, more negative pressure is required to drain a given pore size. As mentioned above, increased salt concentrations can induce greater surface tension.

The amount of water retained at relatively low values of suction (between 0 and 1 bar) depends primarily on the capillary effect and the pore-size distribution and is, therefore, strongly affected by the structure of the sediment. Water retention at higher suction ranges is due increasingly to water adsorption and is, therefore, influenced less by the structure and more by the texture and specific surface of the soil material. According to Gardner (1968), the water content at a suction of 15 bars is fairly well correlated with the surface area of a sediment and would represent ~10 molecular layers of water if it were distributed uniformly over the particles' surfaces.

Moisture-retention characteristics of a sediment or sand may provide indirect information regarding the effects of NaOH on the solid phase. First, if there were changes in the particle-size distribution as a result of either dissolution or precipitation, moisture-retention data would be affected. Increases in the concentration of smaller particles, resulting from precipitation, would tend to increase capillary forces and water adsorption. Second, the presence of higher NaOH concentrations in the sediment's pore water would tend to increase the water tension that, in turn, would increase the capillary forces (see Equation [1]) that, finally, would cause the sediment to hold onto more water at a given applied suction.

Another potentially important effect of a high-ionic-strength solution, such as the waste-glass leachate, is that it can directly affect hydraulic conductivity. Hydraulic conductivity depends on the attributes of the soil and the fluid. The soil characteristics affecting hydraulic conductivity are total porosity, pore-size distribution, and tortuosity. Together, these characteristics describe the pore geometry. The fluid attributes affecting conductivity are fluid density and viscosity. It is possible in theory, and sometimes in practice, to separate hydraulic conductivity (K, L/t) into two factors: intrinsic permeability of the soil (k, L^2) and fluidity (f) of the liquid or gas (1/[L·t]):

$$K = kf. \tag{3}$$

Fluidity is inversely proportional to viscosity:

$$f = \rho g/\eta \tag{4}$$

where ρ is fluid density (m/L^3), g is gravitational acceleration (L/t^2), and η is viscosity (m/L·t). Hence, intrinsic permeability can be defined as:

$$k = K\eta/\rho g. \tag{5}$$

Based on Equations (4) and (5), it should be obvious that, while fluidity varies with composition of the fluid (and with temperature), the permeability is ideally an exclusive property of the porous medium and its pore geometry alone. A very important assumption in Equation (3) is that the fluid and the solid matrix do not interact in such a way as to change the properties of each other. In a completely stable porous medium, the same permeability will be obtained with different mobile phases (e.g., with water, air, oil). As described above, the waste-glass leachate is expected to have significant interactions with the sediment, thereby compromising the use of Equation (3) for this application. However, it is presented here to provide a first approximation of how density and viscosity can alter hydraulic conductivity under ideal conditions.

As will be described, the waste-glass leachate is likely to be dominated by the Na^+ and OH^- ions and is expected to have a higher salt concentration near the glass and a lower salt concentration away from the glass. Table 1 presents selected physical properties of aqueous solutions as a function of NaOH concentration. These data provide a first approximation of the physical properties of the glass leachate and note the ideal changes in the aqueous phase with respect to fluidity and, more directly, hydraulic conductivity. As the NaOH concentration increases, the density and viscosity increase. But as Equation (5) shows, these two properties have opposing effects on fluidity. Increases in density increase fluidity, whereas increases in viscosity decrease fluidity. The kinematic viscosity is a ratio of the viscosity to the density of the fluid. It expresses the shearing-rate resistance of a fluid mass independently of its density. Table 1 shows that the kinematic viscosity increases with NaOH concentration, indicating that fluidity of these solutions decreases (see Equation [4]) and hydraulic conductivity increases (see Equation [3]) with increases in NaOH concentration. Among the important conclusions is that as the ionic strength of the solution increases, the viscosity increases at a faster rate than density. Thus, as indicated by Equations (3) and (4), the hydraulic conductivity would be expected to decrease as the ionic strength decreases. Again, this assumes no liquid-matrix interactions.

Table 1 also shows the relative viscosity, the total concentration of water in a fixed volume (1 L), and the concentration of water displaced from the fixed volume by anhydrous NaOH. The relative viscosity is a ratio of the viscosity of the NaOH solutions to that of water. It shows that the viscosity of the 5-M NaOH solution is more than 3 times greater than that of water. The total water concentration and the concentration of water displaced by anhydrous solutes does not follow a linear trend because of the changes in the long-range and short-range interactions between water molecules and the Na^+ and OH^- ions and the $NaOH^0$ ion pair. Briefly, a small amount of NaOH in water introduces structure to the water molecules, thereby permitting more water to be packed into a given volume. As the concentration of NaOH in solution increases, the effect of increasing structure to the water becomes a secondary effect of the Na^+ and OH^- ions displacing water molecules. These data show that there is more water in a liter of

Table 1. Physical Properties of Water and Aqueous NaOH Solutions[(a)]

NaOH (M)[(b)]	Density, ρ (g/mL)	Viscosity, η (poise or g/cm·s x 10^{-2})	Kinematic Viscosity, η/ρ (centistoke or mL/cm·s)[(c)]	Relative Viscosity, η/η_w (unitless)[(d)]	Total Water Concentration, C_w (g/L)	Water Displaced by Anhydrous Solute, C_0-C_w (g/L)[(e)]
0	0.998	1.002	1.004	1.000	998.2	0
0.5	1.021	1.113	1.090	1.110	1,003	-2.0
1.0	1.043	1.248	1.197	1.246	1,001	-2.9
5.0	1.186	3.344	2.819	3.337	984.5	13.8

(a) Data from Weast (1988 p. D-257) for solutions at 20°C.
(b) 0-M NaOH is deionized water.
(c) Kinematic viscosity is the ratio of viscosity to density, η/ρ.
(d) Relative viscosity is the ratio of the solution viscosity to water viscosity, η/η_w.
(e) Water displaced by anhydrous solute is the difference between the concentration of pure water (C_0) and the water concentration in the salt solution (C_w).

1.0-M NaOH than in pure water, whereas there is appreciably less water in 5.0-M NaOH than in pure water. The important point is that high concentrations of NaOH, as well as other salts, can have large effects on water concentrations.

1.4 Report Outline

In addition to the introduction, objectives, scope, and background, this report describes in Chapter 2.0 the materials and methods used in the two types of experiments. The results and discussion of the experiments are given in Chapter 3.0, followed by the conclusions in Chapter 4.0. The references cited in the text are provided in Chapter 5.0, and an appendix of additional background information and general results is provided.

2.0 Materials and Methods

2.1 Overview

Two experiments were conducted, and the details of the materials and methods for each are described in the sections that follow. Both experiments involved putting either a coarse quartz sand (#2095 Industrial Quartz, Unimin Corporation, Emmett, Idaho) or a Hanford Site composite sediment (E24/E25/E26 sediment) in contact with NaOH solutions (0, 0.01, 0.1, and 1 M NaOH) for 0, 1, 2, or 10 months. The intended media/solution contact time was 12 months. However, both experiments were terminated at the end of 10 months because of algae growth.

The quartz sand was selected to provide information relevant to the capillary-break material that may be used in the engineered barrier around the immobilized glass waste. The quartz sand is expected to provide a worst-case scenario because it has a finer texture than the actual material being considered for the barrier. The greater surface area-to-volume ratio of the quartz sand will tend to accelerate mineral dissolution compared to what would be expected to occur with larger particles of the same mineralogical composition.

The details of the individual sediment cores used in the Hanford Site composite sample are presented in the Appendix (Table A.1). Briefly, this composite sediment was made from all the archived samples (85 individual samples that ranged in depth from 3 to 17 m below ground surface) collected from 3 boreholes. The intent was to create a large mass of homogeneous material with "average" properties representative of backfill material that may be used in the near field of the ILAW-DC. The composite sample will also be used in fiscal year 1999 hydrologic studies that will build on the characterization data generated in these experiments.

The following parameters were measured in the two experiments: saturated hydraulic conductivity, porosity, bulk density, particle-size distribution, moisture retention, K_d, pH, and aqueous cation concentrations. The procedures used to measure these parameters are described in Table 2.

Great care was taken to pack the columns used to measure hydraulic conductivity, porosity, and bulk density. Teflon™ columns, with a length of 12 cm and a diameter of 4.5 cm, were packed as uniformly as possible following the procedure identified in Table 2 (Teflon is a trademark of the Dow Chemical USA, Midland, Michigan). Briefly, ~40 g of dried sediment were poured into the column. The sample was then tamped by hand with a wooden dowel to as high a density as possible. Before adding the next 40-g increment of sediment, the surface of the tamped portion was lightly scratched with a spatula to minimize layering between the 40-g increments. It generally took ~30 min to pack each column. Based on the experimental results, this method was quite satisfactory. The columns were then used with the appropriate NaOH-treatment solution to measure hydraulic conductivity, porosity and bulk density, following the procedures identified in Table 2.

K_d values were measured following the procedure described in Relyea et al. (1980). Cs, Sr, and U(VI) K_d values were measured using the NaOH-treated composite sediment only (not the quartz sand). Three replicates were used for each NaOH/contact-time treatment combination. Cs and Sr K_d experiments were conducted in the same vials, whereas U(VI) experiments were conducted in separate vials. The radionuclides were added to the appropriate NaOH solutions at activities of 15 μCi/L Cs (as $^{137}Cs^{+}$), 15 μCi/L Sr (as $^{85}Sr^{2+}$), and 50 μg/L U(VI) (as $^{238}UO_2^{2+}$). The spikes were placed in deionized water, and no further adjustments for pH were made. The solutions were placed on a platform shaker for 7 days, a period selected to ensure that steady-state conditions were achieved. The effluent solutions were passed though a 0.20-μm filter, and the filtrates were analyzed for total radionuclide activity.

Table 2. Procedures Used in These Experiments

Parameter	Procedure	Procedure/Comments
Particle-size distribution	SA-3 (PNL 1988)	Particle-size analysis (sieve method)
Hydraulic conductivity	SA-4 (PNL 1988)	Falling head hydraulic conductivity
Water retention	SA-6 (PNL 1988)	Water retention; pressure plate and CX-2 methods
Water content	SA-7 (PNL 1988)	Water content; necessary for constant head hydraulic conductivity
Bulk density	SA-8 (PNL 1988)	Clod density/bulk density; necessary for constant head hydraulic conductivity
Particle density	SA-9 (PNL 1988)	Determining particle density; necessary for constant head hydraulic conductivity
Column packing	WHC-IP-0635, GEL-3 Rev. 3	Moisture-density relationship of soils (Section 2.5 for packing column); necessary for constant head hydraulic conductivity
Cation concentrations	ALO-211, Rev. 0 (PNL 1989)	Determination of elements by inductively coupled argon plasma atomic emission spectrometry
pH	G-5-pH (PNL 1989)	Measuring pH of low-level radioactive solutions

An index of the solubility of the radionuclides in the four treatment solutions was estimated.

$$\text{Filtration ratio} = \frac{A_{final}}{A_{initial}} \quad (6)$$

where A_{final} is the radionuclide activity in the <0.20-μm filtrate and $A_{initial}$ is the radionuclide activity added to the NaOH-treatment solution. Sediment was not added to the solutions used to calculate the filtration ratios. The purpose of collecting this information was to help differentiate radionuclide removal from solution by precipitation and adsorption onto labware (i.e., glassware and filters) from radionuclide adsorption onto sediment. If the filtration ratio is <1, then precipitation or container wall adsorption likely occurred.

For the U(VI) K_d determinations, a 10-mL aliquot of the filtered U(VI) solutions was then added to 5 g of dried, NaOH-treated sediment. For Cs and Sr K_d determinations, a 30-mL spiked treatment solution was added to the 1 g of sediment. The solid-to-liquid ratio selection was based on obtaining the maximum sensitivity for the K_d measurement. Because U(VI) has an appreciably lower K_d value than Cs or Sr, a higher solid-to-liquid ratio was used. The spiked sediment suspensions were placed on a slow-moving platform shaker for 14 days. The suspensions were centrifuged, and the supernatants were then passed through 0.45-μm filters. Radionuclide activity in the filtrates was determined.

The K_ds (mL/g) were then calculated.

$$K_d = \frac{(A_{initial} - A_{final}) \times V_{solution}}{A_{final} \times M_{sediment}} \quad (7)$$

where $A_{initial}$ is the initial radionuclide activity in the spike solution (μCi/L; positive control), A_{final} is the radionuclide activity in the effluent solution after equilibration (μCi/L), $V_{solution}$ is the volume of radionuclide solution (mL), and $M_{sediment}$ is the sediment mass (g).

Two types of control treatments were included in the K_d experiments: a negative and a positive. The positive control, containing the radionuclide-spiked solution and no sediment was used to evaluate radionuclide sorption to labware. The negative control contained sediment and groundwater without the added radionuclides and served to account for background activity in the uncontaminated sediment and treatment solutions and to provide information about radionuclide detection interferences during analytical analysis.

Effluent chemical composition was determined using standard techniques. Inductively coupled plasma-atomic emission spectroscopy (ICP-AES), with an analytical precision of ±4% at 5 mg/L, was used to determine dissolved cation concentrations. Ion chromatography, with an analytical precision of ±4% at 5 mg/L, was used to determine dissolved anion concentrations. U(VI) was measured by laser phosphorimetry (Chemchek Instruments, Inc., Richland, Washington; Brina and Miller 1992). The laser phosphorimetry method had a detection limit 0.005 mg/L UO_2^{2+} and an analytical precision of 2% at 0.01 mg/L UO_2^{2+}. Analyses for ^{137}Cs and ^{85}Sr were by gamma energy analysis using a Wallac® 1480

Wizard™ 3-in. NaI automatic gamma detector (EG&G Wallac, Wellesley, Massachusetts). Generally, all counting analytical methods were performed to 3% combined error, with systematic error accounting for <1% of the total error.

2.2 Batch Experiment

The batch experiments consisted of the following treatments: 2 solid-phase materials, 4 NaOH treatments, 4 times, and 2 replicates. Either the quartz sand or the composite sediment (~400 g) and 800 mL of the NaOH solutions were placed in plastic 1-L containers. The plastic 1-L containers were placed on a laboratory bench and mixed twice a week by vigorously shaking for ~1 min. Sixteen containers (2 replicates x 2 materials x 4 NaOH treatments) were sampled at each of 4 contact times: 0, 1, 2, and 10 months. The materials were centrifuged to separate the solids and solution. A <0.45-μm filtrate subsample of the aqueous phase was collected for ICP analysis, and the remainder of the liquid was carefully poured out, being careful not to lose any fine particles. The moist sediment samples were then oven dried at 105°C. The mass of the NaOH salt left in the aqueous phase was accounted for in calculating the particle-size distributions.

Approximately 300 g of very well-mixed dried solids were then packed into 2.5-cm-dia., 12-cm-long, Teflon™ columns. Great care was taken to pack the 48 columns (2 materials x 4 NaOH treatments x 3 contact times x 2 replicates) uniformly and as tightly as possible following the procedure described in Section 2.1. Moisture-retention curves were generated at 6 water potentials, including 0 bar (saturated conditions). These data were collected using the appropriate NaOH-treatment solutions. Particle-size distribution was measured on ~40 g of dried samples, using the dry-sieve method. As will be discussed in Section 3.0, drying the sediments clearly produced an experimental artifact, whereby the particles, on drying, aggregated. To eliminate this artifact, it would have been better to conduct the particle-size distribution analysis via wet sieving (i.e., passing water through the nest of sieves) and to use sediment samples that had not been dried.

2.3 Column Experiment

This experiment had a full factorial design, involving 2 solid-phase materials (quartz sand or composite sediment) and 4 NaOH treatments (0, 0.01, 0.1, and 1.0 M). The eight columns were made of Teflon™ and were 12 cm long and 4.5 cm dia. The columns were carefully packed, as described in Section 2.1. Prior to performing the column experiment, particle-size distribution, water retention, hydraulic conductivity, porosity, and bulk density were measured for both materials. The treatment solutions were introduced at a flow rate of 48 mL/h into the packed columns for 10 months. Periodically, the flow rates, pH values, and cation concentrations of the effluents were measured following standard procedures (see Table 2). At the end of the 10-month treatment period, particle-size distribution, hydraulic conductivity, porosity, bulk density, and K_d values were remeasured.

3.0 Results and Discussion

3.1 Physical Properties

3.1.1 Batch Experiment

The batch experiment consisted of 52 containers in which the quartz sand or the composite sediment were treated with 4 different concentration of NaOH for 3 contact times ([2 solid phases x 2 replicates x 4 NaOH treatments x 3 contact times] + [2 solid-phase controls, no treatment x 2 replicates]). The hydraulic conductivity, bulk-density, porosity, particle-size distribution, moisture-retention, and radionuclide K_d values of these treated samples were measured. The experiment was terminated early, at 10 months, because algae growth became apparent. The intended contact time was 12 months. It is hard to determine what impact the algae had on the 10-month sediment samples. Algae clearly impacted the K_d measurements, as will be discussed, but did not appear to greatly impact the hydrology and physical measurements. For future studies, it may be possible to conduct batch experiments for greater than 10 months if the aqueous phases are spiked with algaecides, the sediment and water are sterilized, or the entire experiment is conducted in the dark at 5°C.

The porosity of the treated quartz sand and composite sediment is presented in Table 3. The variability, as measured by the standard deviation in these measurements, was extremely low, suggesting that the columns used to measure the porosity were packed in a consistent manner. The quartz sand consistently had a porosity of ~0.38 cm^3/cm^3, except for the 1.0-M NaOH treatment measured after 2 months of contact time (0.33 ± 0.01 cm^3/cm^3).

Table 3. Effect of NaOH Concentrations and Contact Time on Porosity (cm^3/cm^3; mean ± standard deviation of two replicates): Batch Experiment

NaOH (M)	Quartz Sand (month)				Composite Sediment (month)			
	0[a]	1	2	10	0[a]	1	2	10
0	0.39 ± 0.01	0.37 ± 0.01	0.38 ± 0.00	0.38 ± 0.01	0.29 ± 0.01	0.28[b]	0.27 ± 0.01	0.29 ± 0.02
0.01	--[c]	0.37 ± 0.00	0.37 ± 0.02	0.39 ± 0.01	--[c]	0.29 ± 0.01	0.28 ± 0.01	0.29 ± 0.01
0.1	--[c]	0.36 ± 0.01	0.37 ± 0.01	0.37 ± 0.03	--[c]	0.29[b]	0.27 ± 0.00	0.29 ± 0.01
1.0	--[c]	0.38 ± 0.01	0.33 ± 0.00	0.38 ± 0.00	--[c]	0.33 ± 0.01	0.29 ± 0.00	0.33 ± 0.00

(a) Untreated.
(b) Not replicated.
(c) Not measured.

The composite sediment had a lower, but also consistent, porosity of ~0.29 cm^3/cm^3. At all three sample times, an increase in sediment porosity was observed as the NaOH concentration increased. This

suggests that some sediment may have dissolved and that this dissolution occurred quickly, prior to the first sampling at 1 month. The porosity of the quartz sand did not change in a consistent manner while in contact with NaOH solutions.

The bulk-density values for the same columns used to measure porosity (see Table 3) are presented in Table 4. Again, the variability for each treatment, as measured by the standard deviation of the mean, was quite low. This indicates that the columns used to measure the bulk density within a treatment were packed in a consistent manner. Prior to any treatment, the bulk density of the quartz sand was 1.56 ± 0.02 g/cm^3 and for the composite sediment was 1.79 ± 0.00 g/cm^3. As the NaOH concentration increased, the bulk density in the composite sediment tended to decrease. As expected, this is consistent with the trend that porosity increased with NaOH-concentration treatment (see Table 3). As was the case with porosity, no consistent trend in bulk-density changes was observed in the quartz sand experiments. All attempts were made to preclude experimental artifacts, and it is believed that the trends in the composite sediment are real.

Table 4. Effect of NaOH Concentrations and Contact Time on Bulk Density (g/cm^3; mean ± standard deviation of two replicates): Batch Experiment

NaOH (M)	Quartz Sand (month)				Composite Sediment (month)			
	0[a]	1	2	10	0[a]	1	2	10
0	1.56 ± 0.02	1.63[b]	1.59 ± 0.01	1.55 ± 0.03	1.79 ± 0.00	1.86[b]	1.84 ± 0.00	1.73 ± 0.03
0.01	--[c]	1.58 ± 0.03	1.58 ± 0.02	1.57 ± 0.00	--[c]	1.83 ± 0.02	1.86 ± 0.06	1.77 ± 0.01
0.1	--[c]	1.60 ± 0.00	1.60 ± 0.01	1.57 ± 0.00	--[c]	1.81 ± 0.01	1.82 ± 0.01	1.75 ± 0.02
1.0	--[c]	1.58 ± 0.03	1.52 ± 0.03	1.55 ± 0.01	--[c]	1.71 ± 0.03	1.78 ± 0.01	1.66 ± 0.03

(a) Untreated.
(b) Not replicated.
(c) Not measured.

Saturated hydraulic conductivity values for the packed columns used to measure porosity (see Table 3) and bulk density (see Table 4) are presented in Table 5. Prior to any treatment, the conductivity of the quartz sand was 4.27 cm/min and the composite sediment was 0.13 cm/min. These values are within the expected range for materials with their textures (Freeze and Cherry 1979). The hydraulic conductivity data for hydroxide-treated materials did not show trends as well-defined as those for the bulk-density and porosity data. For the quartz sand at 1 month, hydraulic conductivity did not change significantly with increased NaOH-concentration treatment; at 2 months, it increased; at 10 months, it decreased (see Table 5). For the composite sediment at 1 and 10 months, the hydraulic conductivity increased with increased NaOH-concentration treatment; at 2 months, no significant trend was observed. Thus, there does not appear to be a clear effect of NaOH treatments on the hydraulic conductivity measured in the quartz sand, whereas there may be an NaOH effect, albeit inconsistent, on the composite sediment. For the composite sediment, the NaOH-concentration treatments increased the hydraulic conductivity as the hydroxide concentration increased.

Table 5. Effect of NaOH Concentrations and Contact Time on Hydraulic Conductivity (cm/min; mean ± standard deviation of two replicates): Batch Experiment

NaOH (M)	Quartz Sand (month)				Composite Sediment (month)			
	0[a]	1	2	10	0[a]	1	2	10
0	4.27 ± 0.21	5.90[b]	9.89 ± 1.01	4.43 ± 0.77	0.13 ± 0.09	0.15[b]	0.10 ± 0.08	0.12 ± 0.06
0.01	--[c]	7.82 ± 1.42	9.54 ± 1.23	2.85 ± 0.09	--[c]	0.20 ± 0.21	0.22 ± 0.31	0.24 ± 0.13
0.1	--[c]	6.48 ± 1.45	8.98 ± 1.30	2.59 ± 1.38	--[c]	0.21 ± 0.24	0.13 ± 0.02	0.40 ± 0.10
1.0	--[c]	5.34 ± 2.71	14.48 ± 0.43	2.69 ± 0.00	--[c]	1.44 ± 0.09	0.07 ± 0.01	0.92 ± 0.03

(a) Untreated.
(b) Not replicated.
(c) Not measured.

The increased hydraulic conductivity may be the result of increased fluidity (see Equation [4]) or to increased dissolution of sediment with increased NaOH concentration. The variability for any given hydraulic conductivity measurement was acceptable, as shown by the standard deviations presented in Table 5. This suggests that the lack of consistency between trends at various contact times was related to the experimental method of applying the treatments.

The particle-size distribution of the quartz sand and the composite sediment before and after treatment with the varying NaOH solutions is presented in Table 6. Some serious measurement artifacts compromised the particle-size distribution data. The measurements were made using dried samples. On drying the samples, some of the fine-grained materials aggregated. Consequently, this resulted in the method incorrectly assigning these fine-grained particles to larger size fractions. Additionally, this problem was more apparent with the composite sediment samples than with the quartz sand. A better procedure would have been to 1) attempt to displace or dilute the salts remaining in the pore spaces prior to conducting the measurement; 2) separate the particles using wet-sieve techniques (flush the nondried solids with water); and 3) use moist, not oven-dried, samples in the analyses. Given this important caveat, the data are presented to provide some idea of the overall trends.

Greater than 90% of the quartz sand existed in two size fractions, the 2- to 1- and the 1- to 0.5-mm fractions (see Table 6). The NaOH treatments appeared to have little effect on the quartz sand's particle-size distribution. This can most easily be seen by comparing the data from the 0- and 1.0-M NaOH treatments after 10 months of contact time. The concentration of the >0.25-mm fraction never accounted for >1% of the total mass.

As expected, the particle-size distribution of the composite sediment was wider than that of the sand. Approximately 90% of the mass existed in the 4 fractions that include sizes between 2 to 0.1 mm (see Table 6). There was little mass in the >2-mm fraction because the sediment had been passed through a 2-mm sieve prior to use in this experiment. The proportion of the finest particles of the 0-M NaOH sediment treatments, <0.002 mm, tended to decrease during the 10-month contact. The proportion of the

Table 6. Effect of NaOH Concentrations and Contact Time on Particle-Size Distribution: Batch Experiment[a]

Contact Time (month)	NaOH (M)	% Particle-Size (mm) Distribution							
		>2	2 to 1	1 to 0.5	0.5 to 0.25	0.25 to 0.1	0.1 to 0.075	0.05 to 0.002	<0.002
Quartz Sand									
0	NT[b]	3.43 ± 0.14	87.53 ± 1.12	8.15 ± 0.65	0.73 ± 0.54	0.15 ± 0.18	0 ± 0	0 ± 0	0 ± 0
1	0	10.86 ± 1.54	81.52 ± 1.95	6.74 ± 0.42	0.12 ± 0.07	0.05 ± 0.03	0.01 ± 0.02	0.01 ± 0.02	0.90 ± 0.72
	0.01	6.92 ± 2.15	84.64 ± 1.06	7.99 ± 1.02	0.16 ± 0.09	0.16 ± 0.02	0.01 ± 0.02	0.01 ± 0.02	0.20 ± 0.07
	0.1	11.47 ± 4.57	79.99 ± 0.68	7.83 ± 3.66	0.34 ± 0.27	0.02 ± 0.00	0.01 ± 0.02	0.00 ± 0.00	0.34 ± 0.05
	1.0	8.83 ± 1.56	83.77 ± 1.31	6.20 ± 0.11	0.07 ± 0.07	0.02 ± 0.00	0.01 ± 0.02	0.01 ± 0.02	1.07 ± 0.03
2	0	10.70	83.93	5.17	0.10	0.05	0.05	0	0
	0.01	11.83	82.14	6.03	0.05	0.05	0	0	-0.09
	0.1	6.72	78.25	14.70	0.29	0	0	0	0.05
	1.0	14.36	81.88	3.63	0.05	0.04	0.02	0	0.02
10	0	8.37 ± 2.79	85.64 ± 1.16	5.97 ± 1.59	0.02 ± 0.04	0 ± 0	0 ± 0	0 ± 0	0 ± 0
	0.01	7.12 ± 0.17	86.49 ± 0.41	6.22 ± 0.54	0.12 ± 0.07	0.02 ± 0.00	0 ± 0	0.01 ± 0.02	0.01 ± 0.02
	0.1	7.29 ± 0.17	86.34 ± 0.45	6.10 ± 0.42	0.15 ± 0.18	0.02 ± 0.04	0.01 ± 0.02	0.03 ± 0.05	0 ± 0
	1.0	9.19 ± 1.84	86.55 ± 1.70	4.16 ± 0.12	0.02 ± 0.00	0.04 ± 0.02	0.01 ± 0.02	0.01 ± 0.02	0.02 ± 0.00
Composite Sediment									
0	NT[b]	0 ± 0	11.83 ± 0.71	33.83 ± 1.65	30.00 ± 0.00	13.50 ± 1.18	3.33 ± 0.47	2.50 ± 0.24	5.00 ± 0.47
1	0	0.06	10.71	39.98	26.06	10.38	2.48	1.10	9.22
	0.01	0.09	10.31	35.21	24.94	12.35	3.20	1.39	12.49
	0.1	0.14	18.34	38.36	26.77	7.23	1.39	0.57	7.18
	1.0	0.10	12.08	38.92	25.38	12.54	2.82	1.06	7.10
2	0	0.28	15.88	36.68	23.20	10.05	2.44	1.41	10.05
	0.01	0.20	11.47	34.11	24.53	13.90	3.62	1.84	10.33
	0.1	0.28	16.59	38.50	23.24	8.53	2.04	1.18	9.63
	1.0	0.22	12.26	34.68	23.74	13.85	3.87	1.80	9.58
10	0	0.19 ± 0.16	23.08 ± 4.12	37.25 ± 1.02	22.39 ± 2.40	8.57 ± 0.66	2.18 ± 0.06	1.48 ± 0.02	4.86 ± 0.20
	0.01	0.15 ± 0.12	23.22 ± 3.30	37.35 ± 2.19	21.83 ± 1.30	8.46 ± 1.83	2.22 ± 0.65	1.51 ± 0.39	5.26 ± 1.44
	0.1	0.40 ± 0.19	20.62 ± 5.46	37.07 ± 2.91	22.59 ± 2.00	9.22 ± 2.77	2.41 ± 1.01	1.66 ± 0.66	6.02 ± 2.11
	1.0	0.42 ± 0.40	27.00 ± 7.15	38.07 ± 1.49	20.68 ± 2.77	7.60 ± 2.93	1.93 ± 1.18	1.28 ± 0.83	3.02 ± 1.34

(a) Fine particles aggregated as a result of drying the sediment samples. This resulted in an underestimation of the true concentration of finer particles and an overestimation of larger particles. Either one or two (with standard deviations) replicates of these measurements were conducted.

(b) NT = No treatment, particle-size distribution of quartz sand and composite sediment prior to any treatment.

finest and the largest particle classes for the composite sediment for the 1.0-M NaOH treatments tended to increase during the 10-month contact. But taking into consideration the standard deviation of the means, there did not appear to be any significant difference between the 0- and 1.0-M NaOH treatments at 10 months.

In general, it appears that the particle-size distribution was rather insensitive, and thus not useful for evaluating the impact of NaOH on the quartz sand and composite sediment. As will be shown in Section 3.2.2, the 1.0-M NaOH treatments caused a dramatic increase in dissolved Si concentrations, indicating that some dissolution did, in fact, take place. Additionally, indirect evidence based on porosity (see Table 3), bulk density (see Table 4), and, to a lesser extent, hydraulic conductivity (see Table 5) also suggests that dissolution of the composite sediment occurred in the 1.0-M NaOH treatment. However, the dissolution could not be observed as changes in particle-size distribution. Sensitivity could be improved by 1) using more sample to improve sensitivity to slight weight changes in the fine samples (40 g were used in this experiment), 2) including more replicates to decrease variability, and 3) examining smaller particle-size fractions (i.e., fractions that are smaller than 0.002 mm). These smaller fractions tend to have a large impact on aqueous chemistry because of their high surface-to-volume ratio. Additionally, the high surface-to-volume ratio tends to make them especially vulnerable to dissolution.

Moisture-retention measurements were also collected for selected NaOH treatments (Figures 1 and 2 and Table A.2 in the Appendix). These data describe how much water a porous solid retains as a function of water potential (suction) imposed on it. Thus, the greater the applied water potential, the less water retained by the sediment.

Moisture retention was measured to provide indirect evidence as to whether dissolution or precipitation occurred and to measure the impact of higher salt concentrations on water retention (the "salt effect") (discussed in Section 1.3). If there were a change in the particle-size distribution as a result of either dissolution or precipitation, moisture-retention data would be affected. Increases in the concentration of smaller particles resulting from precipitation would tend to increase capillary forces and water adsorption. The opposite would occur if the concentration of finer particles decreased as a result of dissolution. Regarding the salt effect, the presence of higher NaOH concentrations in the sediment would tend to increase the water tension that, in turn, would increase the capillary forces that, finally, would cause the sediment to hold onto more water at a given applied suction.

For this experiment, there were few differences between the moisture-retention curves for the quartz sand with the various treatments (see Figure 1[A]). This is consistent with the porosity, bulk-density, hydraulic conductivity, and particle-size distribution data presented above. The moisture content of the quartz sand tended to drop off very quickly once a small potential was applied. This is consistent with the fact that the pores are relatively large and uniform, and once these pores emptied, only a small amount of water remained in the sediment. The 1.0-M NaOH-treated quartz sand at 1 and 10 months (bat 1 M/1 mo and bat 1 M/10 mo in Figure 1[B]) retained more moisture than the 0-M NaOH-treated quartz sand. This could be the result of either the presence of higher electrolyte concentrations (the salt effect) or the presence of smaller particles in the 1.0-M NaOH-treated quartz sand. It seems more likely that the greater moisture retention in the 1.0-M NaOH treatments is due to the salt effect rather than to precipitation because the porosity, bulk-density, and hydraulic conductivity data provide no indication for precipitation.

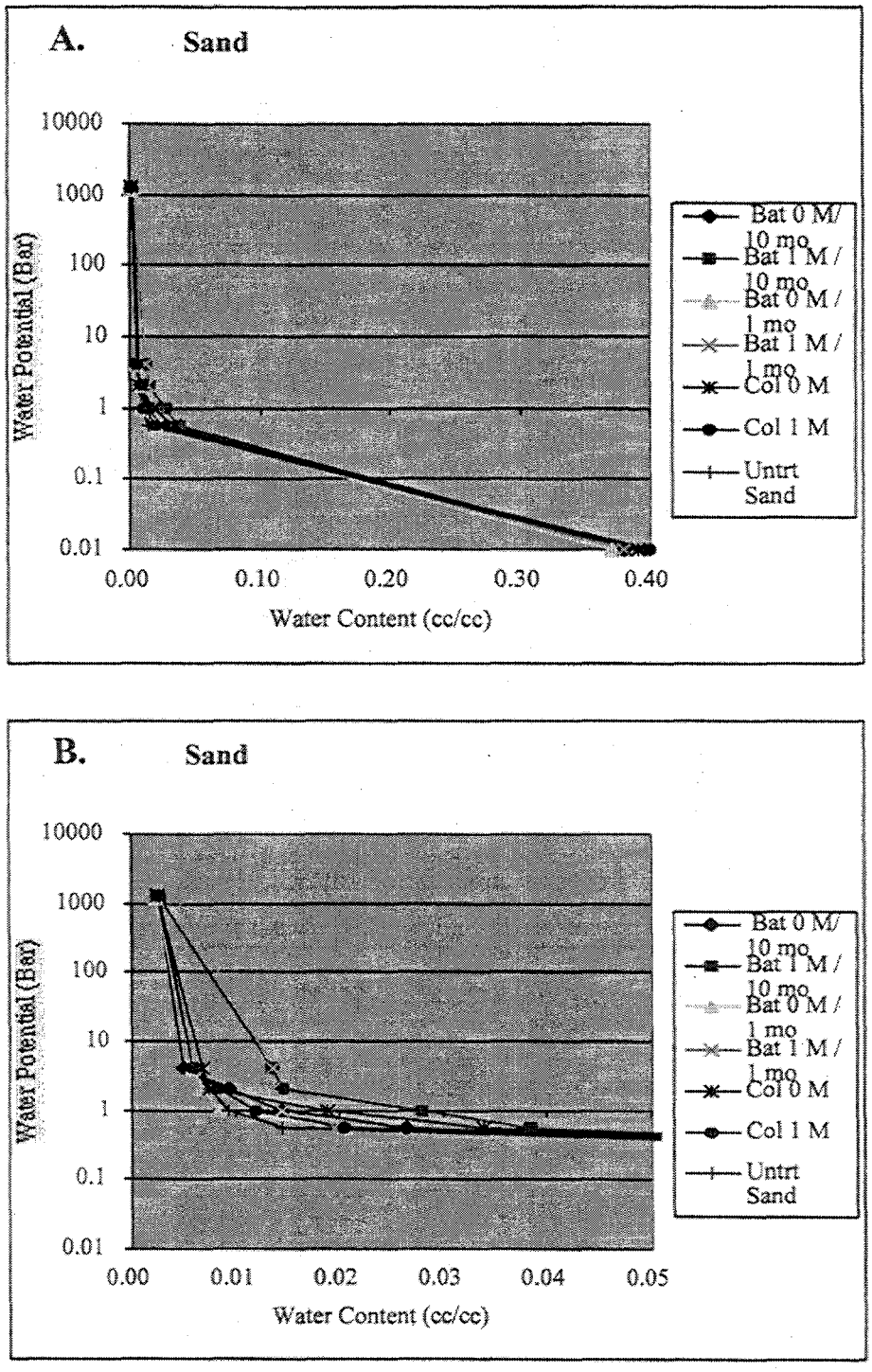

Figure 1. Moisture-Retention Curves for Batch (Bat) and Column (Col) Experiments Conducted with Quartz Sand in Contact with 0 and 1 M NaOH for 0, 1, or 10 Months (mo) (column experiment conducted for 10 mo and untreated sand [Untrt Sand]). A. Entire Data Set. B. Data for <0.05 cm^3/cm^3 Water Content.

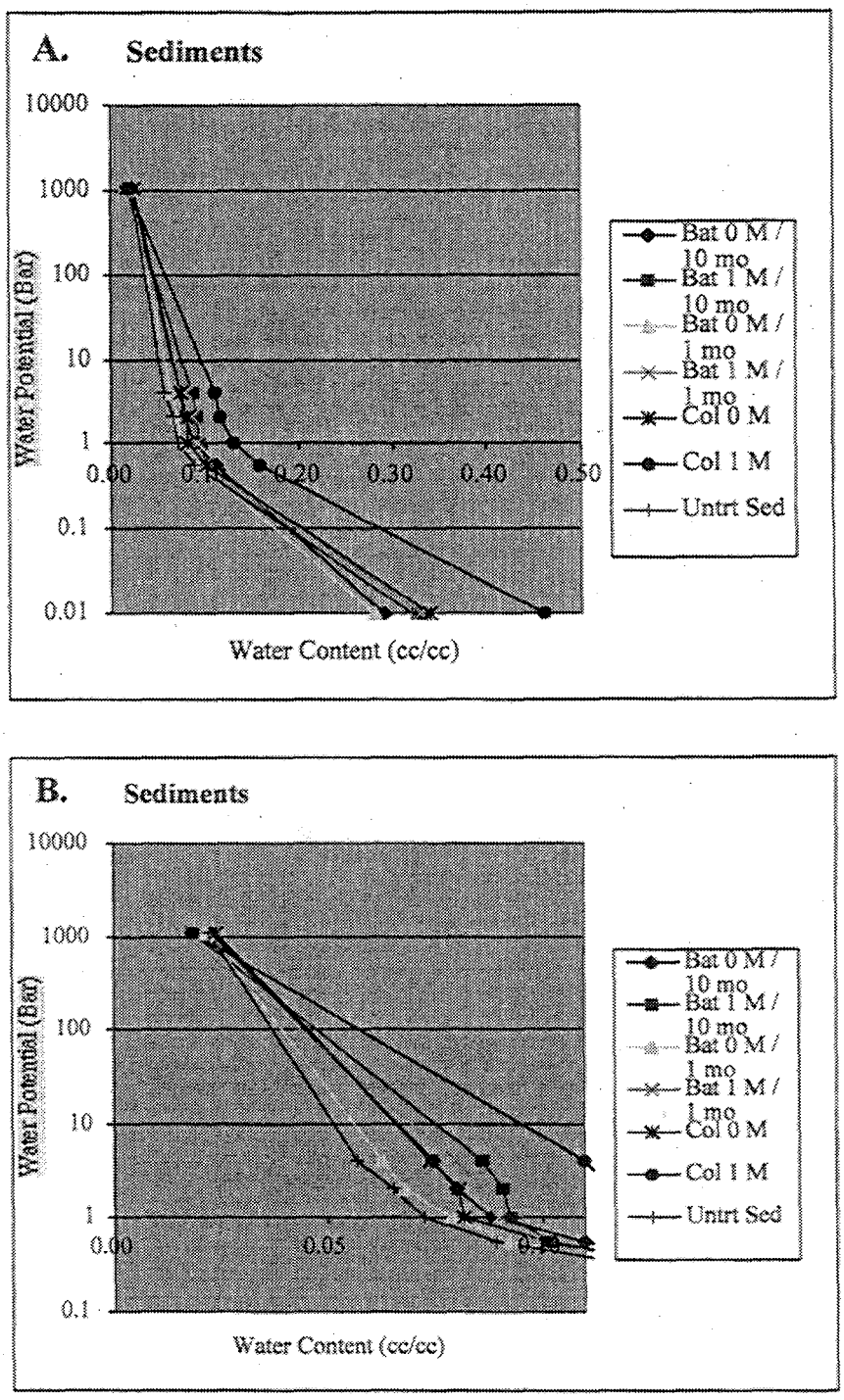

Figure 2. Moisture-Retention Curves for Batch (Bat) and Column (Col) Experiments Conducted with Composite Sediment in Contact with 0 and 1 M NaOH for 0, 1, or 10 Months (mo) (column experiment conducted for 10 mo and untreated sand [Untrt Sed]). A. Entire Data Set. B. Data for <0.11 cm^3/cm^3 Water Content.

If anything, these data show no change in particle-size distribution with perhaps a small amount of dissolution. The column data for the 1.0-M NaOH treatments, shown in Figures 1 and 2 as (Col 1 M), will be discussed below.

As expected, the composite sediment retained more water than the quartz sand at any given applied suction (see Figures 1 and 2). Also, the treatment effects on moisture retention were more pronounced in the composite sediment than in the quartz sand. At 1 and 10 months, the 1.0-M NaOH-treatment samples (bat 1 M/1 mo and bat 1 M/10 mo in Figure 2) tended to retain more water than their respective 0-M NaOH treatments (bat 0 M/1 mo and bat 0 M/10 mo in Figure 2). The fact that the difference between the 0- and 1.0-M NaOH treatments did not change much at the 1- and 10-month samplings indicates that the effect of the NaOH did not change during the 1- and 10-month sampling. Again, the cause for this increased moisture retention is likely the result of the salt effect. There was no evidence that fine particles were formed during the NaOH treatments, whereas there is significant evidence that dissolution occurred.

3.1.2 Column Experiment

Eight columns were set up to evaluate, under dynamic flow conditions, changes in the same hydrologic and physical parameters evaluated in the batch experiment (see Section 3.1.1). After 10 months, the column experiment was terminated, and the particle-size distribution, hydraulic conductivity, bulk density and porosity were measured. As was the case for the batch experiment, algae started to grow in the columns after 10 months. Therefore, the column experiments, originally designed to last for 12 months, were terminated. The algae had a significant, detrimental effect on the K_d measurements. Algae's impact on the physical and hydrologic measurements, presented in this section, appears to be minimal. This is based on comparisons of the column experiment results with those from the batch experiments and data trends for measurements taken when no algae was present (at 1 and 2 months).

As the NaOH concentration was increased, the hydraulic conductivity, and to a lesser extent the porosity, increased for both the quartz sand and composite sediment (Table 7). The bulk density did not change in a consistent manner with respect to NaOH-concentration treatment. In the batch experiments, the composite sediment, but not the quartz sand, showed similar trends, wherein the porosity and hydraulic conductivity increased in samples treated with high concentrations of NaOH (see Tables 3 and 5). The bulk-density values for the composite sediment columns decreased (see Table 7), consistent with the results of the batch experiment (see Table 5).

As discussed in Section 3.1.1, the particle-size distribution measurements for the quartz sand and composite sediment from the column experiment were compromised because of particle aggregation from drying the sediment prior to analysis. Given this important caveat, the data are presented to provide the reader with some general trends.

There was a slight decline from 5.11 % to 3.91% in the amount of solids in the finest fraction (<0.002 mm) for the composite sediment as the NaOH concentration increased. This trend was not as well-defined in the batch experiments but was largely true for all three contact times (see Table 6). No significant differences were noted in the particle-size distributions for the quartz sand. Based on these

Table 7. Effect of NaOH Concentrations on Conductivity, Bulk Density, and Porosity: Column Experiment

NaOH (M)	Conductivity (cm/min)	Bulk Density (g/cm^3)	Porosity (cm^3/cm^3)
Quartz Sand			
0	8.70	1.64	0.39
0.01	9.42	1.67	0.37
0.1	9.86	1.67	0.38
1.0	10.15	1.67	0.40
Composite Sediment			
0	0.24	1.87	0.34
0.01	0.16	1.81	0.38
0.1	0.12	1.82	0.39
1.0	0.55	1.72	0.46

data alone, it is not possible to determine whether the cause for the decrease in the fine-grained particles is due to greater aggregation of the fines in the high-salt treatments or to the dissolution of the fines in the high-salt treatments. But, based on the hydraulic and physical properties presented in Table 8, it appears likely that the decrease in the fine-grained particles is due to dissolution.

Table 8. Effect of NaOH Concentrations on Particle-Size Distribution: Column Experiment[(a)]

NaOH (M)	% Particle-Size (mm) Distribution							
	>2	2 to 1	1 to 0.5	0.5 to 0.25	0.25 to 0.1	0.1 to 0.075	0.05 to 0.002	<0.002
Quartz Sand								
0	6.15	86.02	7.45	0.30	0.05	0	0	0.03
0.01	5.78	85.81	8.01	0.30	0.05	0	0.03	0.03
0.1	5.54	85.07	8.54	0.65	0.12	0	0.05	0.02
1.0	5.95	86.06	7.46	0.38	0.08	0	0.03	0.05
Composite Sediment								
0	0.43	20.52	38.27	22.32	9.54	2.20	1.60	5.11
0.01	0.47	22.36	36.60	21.82	9.68	2.24	1.74	5.11
0.1	0.43	23.82	37.82	21.05	8.61	2.00	1.37	4.87
1.0	0.70	24.26	38.09	21.22	8.59	1.94	1.30	3.91

(a) During the sieve analysis, fine particles were observed to aggregate. This will result in an underestimation of the true concentration of fine particles and an overestimation of the larger particles. One replicate for each measurement was conducted.

The moisture-retention characteristics of the quartz sand and composite sediment treated with 0- and 1.0-M NaOH were presented in Figures 1 and 2. There was no noticeable difference between the 0- and 1-M NaOH data for the quartz sand (see Figure 1[B]), whereas there was a significant difference between these treatments for the composite sediment (see Figure 2[B]). As discussed above, the cause for the difference is likely due to the salt effect.

3.2 Chemical Properties

3.2.1 Batch Experiment

The batch experiments consisted of the following treatments: 2 solid-phase materials, 4 NaOH treatments, 4 times, and 2 replicates. Approximately 400 g of either the coarse quartz sand or the composite sediment and 800 mL of the NaOH solution were placed in plastic 1-L containers. The suspensions were placed on a laboratory bench and mixed twice a week by vigorously shaking for ~1 min. At 1, 2, and 10 months, 16 containers (2 replicates x 1 solid-phase material x 4 NaOH treatments) were studied. The moist solids were then oven dried at 105°C. The NaOH-treated composite sediment was then used in Cs, Sr, and U(VI) K_d measurements. Three replicates of these measurements were made.

The U(VI) K_d values could not be measured by laser phosphorimetry. Apparently, the high pH of the 0.1- and 1.0-M NaOH treatments adversely affected the ability of the complexing agent used in the analysis to complex the UO_2^{2+} species. The activities of these samples were too low to count using radiochemical techniques. Thus, the samples will be analyzed in fiscal year 1999 by the comparatively expensive ICP-mass spectrophotometer (MS) method. Another problem that occurred during these studies was that after 10 months, algae growth became apparent. This greatly compromised the measured K_d values. The algae sorbed large quantities of Cs and Sr, producing K_d values that were 2 to 10 fold greater than expected. The K_d values of the 10-month contact-time samples were measured but not reported.

The filtration ratio (see Equation [3]), a ratio of the Cs and Sr activities before and after passing the contact solutions through a 0.20-μm filter, provides an index of the extent that radionuclides precipitated out of solution or adsorbed to the labware. The filtration ratios are presented in Table 9. The filtration ratios for the 0.01-, 0.1-, and 1.0-M NaOH solutions were approximately equal to unity. The filtration ratio of the 0-M NaOH solution was substantially less than unity, suggesting that Cs and Sr had adsorbed to the labware. An evaluation was made to determine if 0.001-M $NaClO_4$ could be used to replace the 0-M NaOH as a background electrolyte for the measurement of the Cs and Sr K_d values for the 0-M NaOH treatments. It was expected that Na would compete with the Cs and Sr for adsorption sites on the labware. The filtration ratios for the 0.001-M $NaClO_4$ solution was also less than unity (see Table 9). Consequently, the Cs and Sr K_d values measured with either 0-M NaOH or 0.001-M $NaClO_4$ background solutions were difficult to interpret and were, therefore, not reported.

Cs K_d values decreased as the NaOH concentrations increased (Table 10). This trend occurred at all three contact times: 0, 1, and 2 months. The likely cause for this trend is the increased concentration of the competing cation, Na. As more Na was introduced into the system, the competition by the Na for Cs

Table 9. Filtration Ratios (from Equation [3]) of Cesium and Strontium

Background Electrolyte	Cs	Sr
0 M NaOH	0.64	0.69
0.01 M NaOH	1.07	0.93
0.1 M NaOH	1.11	1.00
1.0 M NaOH	1.07	1.03
0.001 M $NaClO_4$	0.69	0.86

Table 10. Cesium K_d Values (mL/g) for Composite Sediment as a Function of NaOH Concentration and Contact Time[a]

NaOH (M)	Contact Time[b] (month)			
	0	1	2	10[c]
0	[d]	[d]	[d]	NA
0.01	3,117 ± 193	3,156 ± 39	3,721 ± 2369	NA
0.1	1,982 ± 330	2,276 ± 186	2,085 ± 1339	NA
1.0	1,017 ± 75	1,167 ± 60	982 ± 191	NA

(a) After the assigned NaOH contact time of 0, 1, 2, or 10 months, K_d values were measured. Radionuclide contact time with NaOH-treated sediment was 14 days; solid: liquid ratio was 1:30; initial ^{137}Cs activity was ~25 μCi/L; appropriate NaOH solutions used as background electrolyte.

(b) Contact time refers to period that the NaOH solutions were in contact with the sediment prior to K_d measurement.

(c) The 10-month K_d data are not reported because algae had grown in the sample containers.

(d) There was substantial evidence that appreciable amounts of the Cs added to the 0-M NaOH solution had adsorbed to labware. Filtration ratios were <1 (see Table 9).

adsorption sites increases, and consequently, the lower the measured Cs K_d value. It is believed that this is a competing ion effect, and not an effect from the dissolution of particles, because the trend was observed in the samples with a contact time of 0 month. The 0-month samples were in contact with NaOH during the 14-day K_d measurement, so it is possible, but not likely, that the full extent of dissolution would take place during this short contact period.

There was a slight increase in Cs K_d values with contact time for the 0.01- and 0.1-M NaOH treatments (see Table 10). The opposite trend was observed for the 1.0-M NaOH treatment. However, there was a great deal of variability in the Cs K_d measurements. The high variability for Cs K_d values has been observed previously in measurements made in the composite sediment (Parker 1997, Kaplan et al. 1998d). This is likely attributed to a nonuniform distribution of 2:1 minerals (such as smectite and illite),

which have extremely high sorption affinity of Cs. Ames and Rai (1978) reported Cs K_d values of 4,900 mL/g for smectite and 2,200 mL/g for illite. Thus, only a very small difference in the distribution of these strongly sorbing minerals in subsamples may cause large variances in Cs K_d values for a given sample. Consequently, large differences in K_d means were needed to observe statistically significant differences. For example, though the K_d values tended to increase for the 0-M NaOH treatment as contact time increased, the correlation was not significant at the 5% level of probability. Similarly, though the K_d values tended to decrease for the 1.0-M NaOH treatment as contact time increased, the correlation was not significant at the 5% level of probability.

The Sr K_d values measured using the composite sediment treated with varying concentrations of NaOH for 0, 1, and 2 months are presented in Table 11. In general, the K_d values are on the high side expected for the composite sediments (Ames and Serne 1991). In environments with low-dissolved organic matter and low-salt concentrations, the range of Sr K_d values estimated by Ames and Serne was 20 to 200 mL/g. Sr K_d values for solutions with high-salt concentrations were estimated by Ames and Serne to be even lower. However, values as high as 2,000 mL/g have been measured in other carbonate-dominated sediments similar to Hanford (Kaplan et al. 1998a). The cause for the unusually high-K_d values reported in Table 11 may be attributed to the relatively high concentration of fine materials in this sediment, ~5% (see Table 6). The greater concentration of fine-grained material provided greater surface area for the Sr to adsorb to.

Table 11. Strontium K_d Values (mL/g) for Composite Sediment as a Function of NaOH Concentration and Contact Time[a]

NaOH (M)	Contact Time[b] (month)			
	0	1	2	10[c]
0	[d]	[d]	[d]	NA
0.01	1,423 ± 123	1,291 ± 173	1,335 ± 410	NA
0.1	311 ± 38	508 ± 39	390 ± 139	NA
1.0	275 ± 17	358 ± 45	339 ± 32	NA

(a) After the assigned NaOH contact time of 0, 1, 2, or 10 months, K_d values were measured. Radionuclide contact time with NaOH-treated sediment was 14 days; solid:liquid ratio was 1:30; initial ^{85}Sr activity was ~33 μCi/L; appropriate NaOH solutions used as background electrolyte.
(b) Contact time refers to period that the NaOH solutions were in contact with the sediment prior to K_d measurement.
(c) The 10-month K_d data are not reported because algae had grown in the sample containers.
(d) There was substantial evidence that appreciable amounts of the Sr added to the 0-M NaOH solution had adsorbed to labware. Filtration ratios were <1 (see Table 9).

The Sr K_d values changed in a consistent and systematic manner with the NaOH-concentration treatments. For all three contact times, the Sr K_d values tended to decrease with increasing NaOH concentration. This trend was also seen with Cs K_d values, albeit the trend was less apparent with the Cs K_d values (see Table 10). Again, the cause for this trend is likely that the added Na competed with Sr for adsorption sites on the sediment surface. There were no systematic changes in Sr K_d values with contact time.

After the appropriate contact time, but prior to measuring K_d values, subsamples of the aqueous phases from the batch experiment were collected, passed through a 0.20-μm filter, and then analyzed by ICP-AES for major cation concentrations. Results from these analyses are presented in the Appendix (Table A.3), and the more interesting trends are presented and discussed below.

The Si concentrations in the various NaOH solutions in contact with the quartz sand in the batch experiment increased as the concentration of the NaOH increased (Figure 3). For the 0-, 0.01-, and 0.1-M NaOH treatments, the solution concentration of Si did not change appreciably between 1 and 10 months of contact time, suggesting that a steady-state condition had been reached within 1 month. The ranges of the Si concentrations were the following: 0-M NaOH, 3.6 to 8.6 mg/L; 0.01-M, 26 to 28 mg/L; 0.1-M, 45 to 53 mg/L; 1.0-M, 127 to 189 mg/L. However, the Si concentrations in the 1.0-M treatment solution did not reach steady state within the 10-month experiment. There are a number of reasons why the high-NaOH treatment did not reach steady state, including that the higher pH levels of these systems were not yet in steady state with the $CO_2(g)$ in the air. The Si could have come into solution through ion exchange, ligand exchange, or dissolution of the quartz. The extent of ion exchange on quartz is very low, thus the majority of the Si, especially at higher NaOH-concentration treatments, must have entered into solution via dissolution.

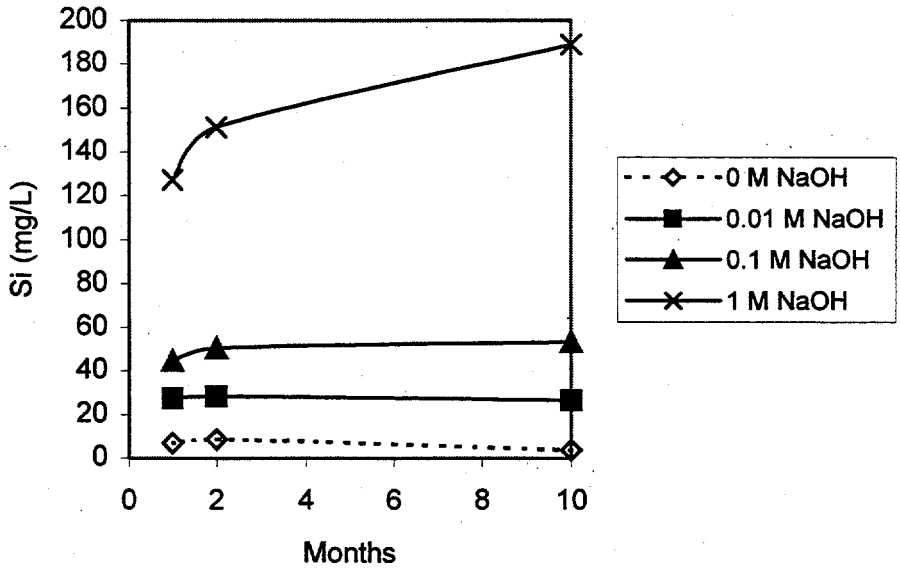

Figure 3. Effect of NaOH Concentrations on Silicon Concentrations in Batch Suspensions Containing Quartz Sand (each data point represents the mean of two observations)

The Si concentration trends for the composite sediment batch experiment effluents (Figure 4) was similar to those observed for the quartz sand in Figure 3. However, appreciably higher Si concentrations were measured in the composite sediment solutions. This likely occurred because the sediment contained appreciable amounts of amorphous silicates and other Si-containing minerals with higher solubility levels in NaOH than quartz. Additionally, the composite sediments contained appreciable amounts of fine-grained materials (see Table 6). Fine-grained materials are more likely to dissolve because of their greater surface area-to-volume ratio than larger particles of the same composition. The Si concentrations in composite sediment effluents reached steady state for the three lower NaOH-concentration treatments. Specifically, the Si concentrations in the 0-, 0.01-, and 0.1-M NaOH treatments were ~25, 40, and 350 mg/L, respectively. For the 1.0-M NaOH treatment, the Si concentrations in the composite sediment did not reach steady state during the 10-month contact period. The Si concentrations increased in the 1.0-M NaOH treatment from 1,282 to 1,944 mg/L between 1 and 10 months of contact.

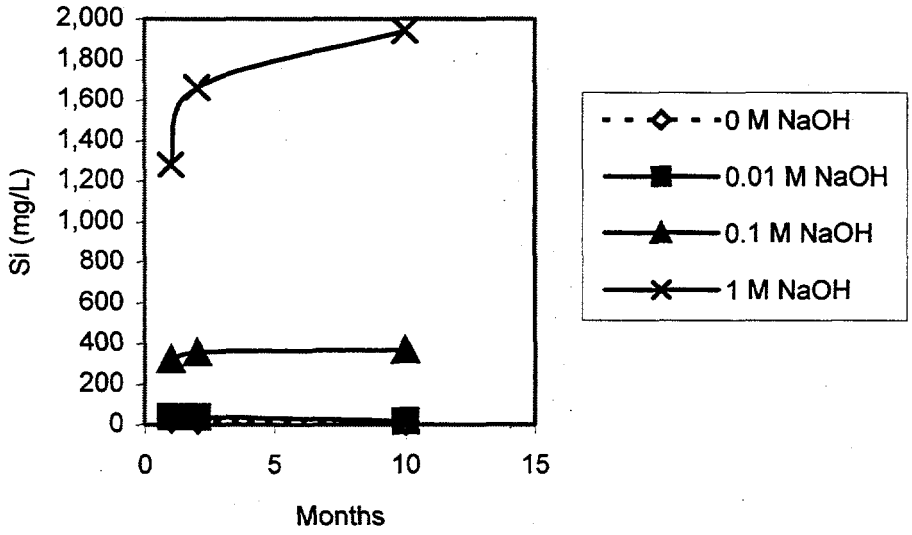

Figure 4. Effect of NaOH Concentrations on Silicon Concentrations in Batch Suspensions Containing Composite Sediment (each data point represents the mean of two observations)

The aluminum concentrations were also elevated in the composite sediment experiments treated with NaOH, indicating that not only silicates but also aluminosilicates were dissolving (see Table 5). Although it is difficult to observe in Figure 5 because of the scale of the plot, Al concentrations increased consistently with increased NaOH concentrations (see Appendix, Table A.3 for details). The Al concentrations were the following: 0-M NaOH, 0.02 to 0.07 mg/L; 0.01-M NaOH, 0.39 to 0.47 mg/L; 0.1-M NaOH, 1.67 to 7.18 mg/L; 1.0-M NaOH, 100 to 135 mg/L. In conclusion, based on the Si and Al concentration data presented in Figures 3, 4, and 5, it is clear that dissolution of composite sediment, and to a lesser extent quartz sand, occurred during these experiments. Evidence for dissolution from the physical and hydrologic parameters discussed in Section 3.1 were not as compelling as from the aqueous chemical composition data presented here.

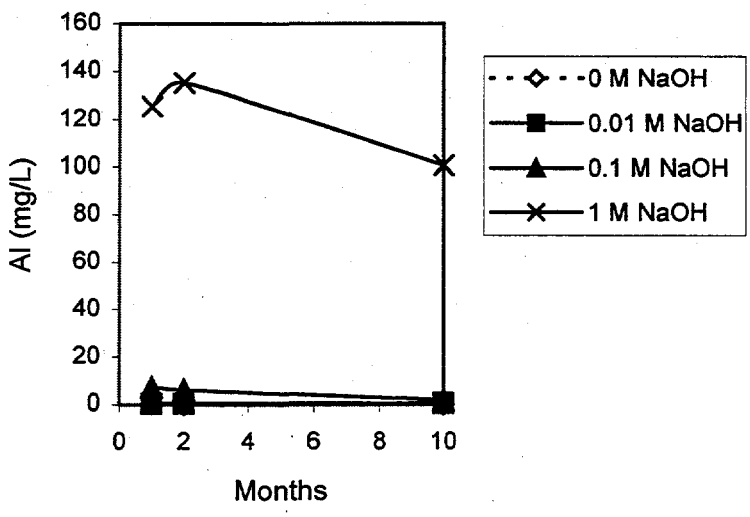

Figure 5. Effect of NaOH Concentrations on Aluminum Concentrations in Batch Suspensions Containing Composite Sediment (each data point represents the mean of two observations)

3.2.2 Column Experiment

Eight columns were set up to evaluate, under dynamic flow conditions, changes in physical and hydrologic parameters similar to the batch experiment (see Section 3.1.1). After 10 months, the column experiment was terminated because algae started growing. The algae had a significant, detrimental effect on the K_d measurements; therefore, the measured K_d values are not reported.

Effluent was collected from the columns, passed through a 0.20-μm filter, and analyzed for cation concentration by ICP-AES. Results from these analyses are presented in the Appendix (Table A.4) and the more interesting trends are presented in the following discussions.

The dissolved Si concentrations in the quartz sand column effluent (Figure 6) were comparable to those in the solutions in contact with the quartz sand in the batch experiment (see Figure 3). This suggests that the column effluent, which flowed at a rate of 45 mL/d or ~1.7-day residence time for each pore volume, was at or near steady state (i.e., the dissolution rate of Si was quite rapid and reached steady state within 1.7 days). For the three lowest NaOH-concentration treatments, the Si concentrations did not vary greatly. As the NaOH-concentration treatment increased, the Si concentration increased incrementally.

Boron can be used as a measure of the degree of congruent dissolution of silicates (Ribbe 1980). The B concentration in the quartz sand column effluent (Figure 7) followed nearly identical trends to those observed for the Si concentrations (see Figure 6). As the NaOH-concentration treatment increased, the B concentrations in the effluent increased incrementally. For the 1.0-M NaOH-concentration treatment

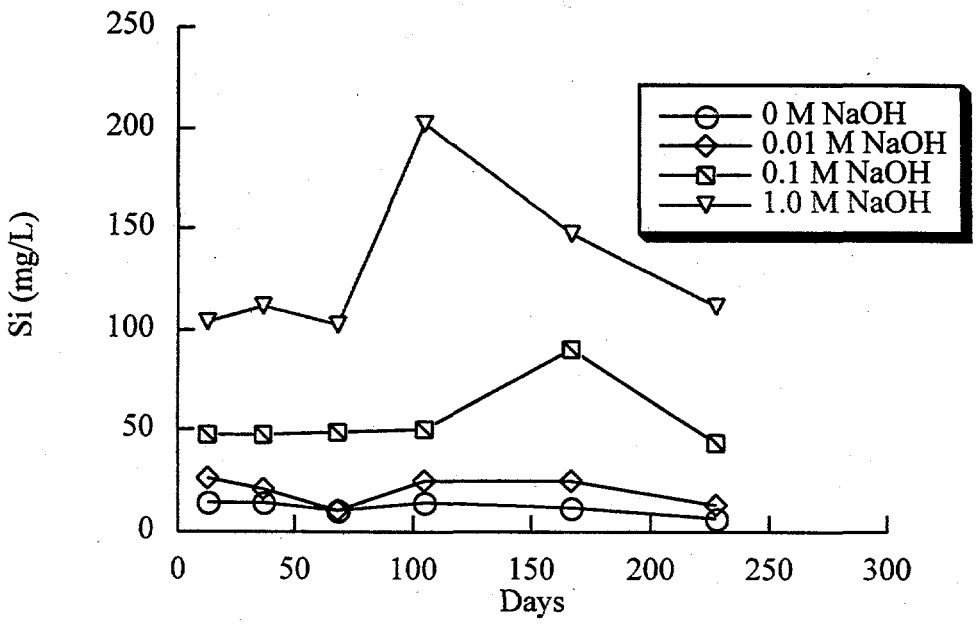

Figure 6. Effect of Influent NaOH Concentrations on Silicon Concentrations in Quartz Sand Column Effluent (each data point represents the mean of two observations)

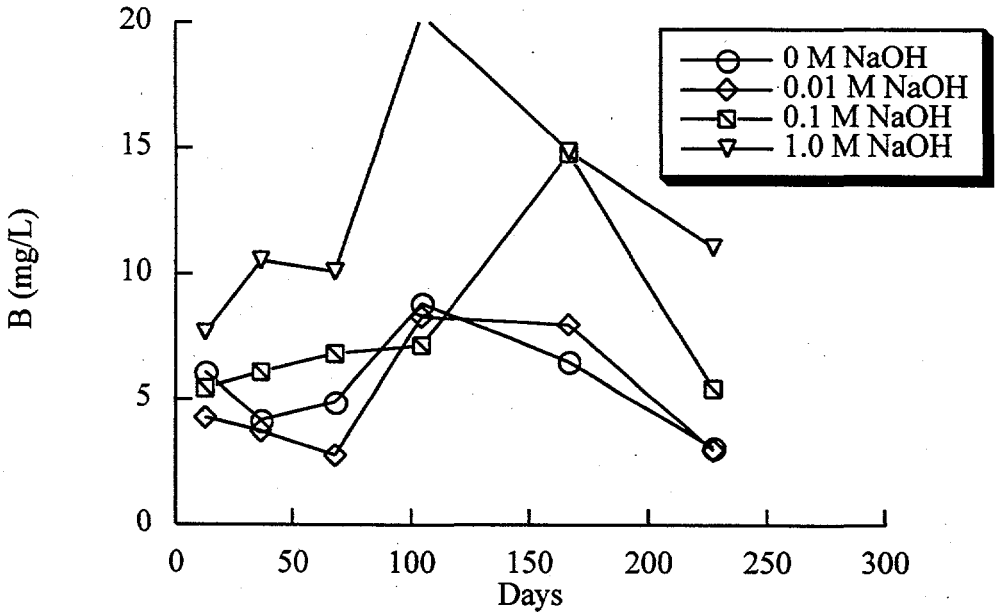

Figure 7. Effect of Influent NaOH Concentrations on Boron Concentrations in Quartz Sand Column Effluent (each data point represents the mean of two observations)

effluent, there was an increase in Si and B concentrations at 100 days followed by a decline in concentrations for the next 2 sampling dates. The similarity of the B and Si concentrations suggests that the Si dissolved congruently and likely did not reprecipitate as a secondary mineral phase. The cause for the increase, followed by the decrease in B and Si concentrations in the 1.0-M NaOH treatment, is not known. It is possible that there was an initial dissolution of comparatively more-soluble Si-containing mineral and that this dissolution process was not immediate but required 60 days of contact with the NaOH solution (i.e., the dissolution process was kinetically hindered with respect to the contact time evaluated). Once the more-soluble phases were dissolved, the Si concentrations decreased. Algae uptake may also be responsible for the decline in Si and B but this is not as likely. Algae growth was not apparent until ~300 days, and there was no similar decline in Fe concentrations (data presented below), an element that algae take up in greater concentrations than either B or Si.

Turning to the effluent from the composite sediment columns, the Si concentrations in the two lowest NaOH-concentration treatments (Figure 8) were comparable to those in the batch experiment (see Figure 4). The two highest NaOH-concentration treatments for the composite sediment column experiment had lower Si concentrations than the sediment batch experiments. This may be caused by kinetic hindrance of the dissolution process under dynamic flow conditions (i.e., the column system was not in chemical steady state). Again, the cause of the decrease of Si concentration in the later samplings of the composite sediment columns is likely caused by an initial dissolution of comparatively more-soluble Si-containing minerals, and once the more-soluble phases were dissolved, the effluent Si concentrations decreased.

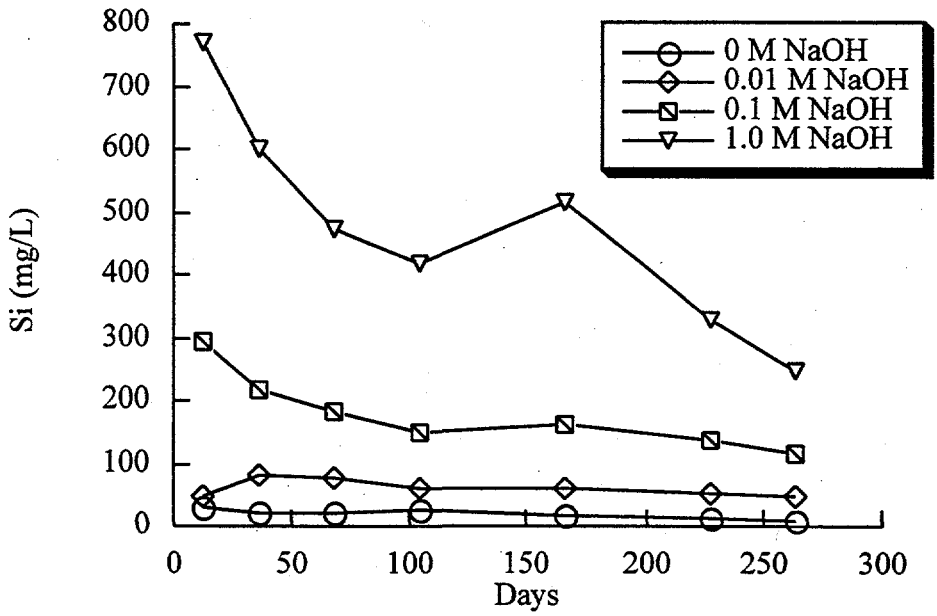

Figure 8. Effect of Influent NaOH Concentrations on Silicon Concentrations in Composite Sediment Column Effluent (each data point represents the mean of two observations

The composite sediment column effluent concentrations of Al, Fe, and K are presented in Figures 9, 10, and 11, respectively. Interpretation of the Al data is especially difficult because of the strong propensity of Al to precipitate as hydroxides and to form polynuclear species at elevated pH. Aluminum exists in natural sediments, primarily in aluminosilicate minerals, and to a lesser extent as adsorbed/precipitated species and gibbsite [$Al(OH)_3$]. As was the case with Si, the Al effluent concentrations from the sediment column were less than those in the batch experiment (see Figure 5). The Al concentrations in the column effluents from the three lowest NaOH-concentration treatments remained relatively constant during the 264-day sampling period, incrementally increasing as the NaOH concentration increased. It is especially interesting to note that NaOH concentrations as low as 0.01 M induced the release of a substantial amount of Al into the aqueous phase. The Al came into the aqueous phase either by mineral dissolution or, to a much smaller extent, by Al ion exchange from the solids. The Al concentrations in the highest NaOH-concentration treatment decreased at the final sample period, 264 days. This trend may have been the result of the initial dissolution of more-soluble Al-containing minerals, followed by the dissolution of less-soluble Al-containing minerals.

Iron exists in Hanford Site vadose-zone sediments primarily as Fe oxide coatings on mineral surfaces. Fe also exists as adsorbed species and in the structures of aluminosilicates, such as illites and smectites. Fe was released from the composite sediment columns only in the highest NaOH-concentration treatment (see Figure 10). For the most part, Fe concentrations for each NaOH-concentration treatment remained essentially constant during the 264-day sample period.

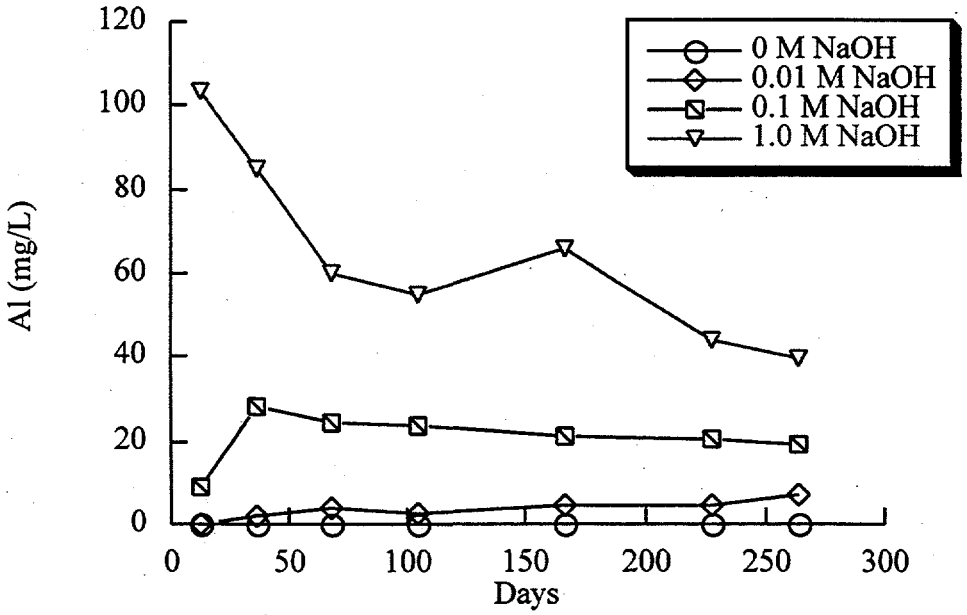

Figure 9. Effect of Influent NaOH Concentrations on Aluminum Concentrations in Composite Sediment Column Effluent (each data point represents the mean of two observations)

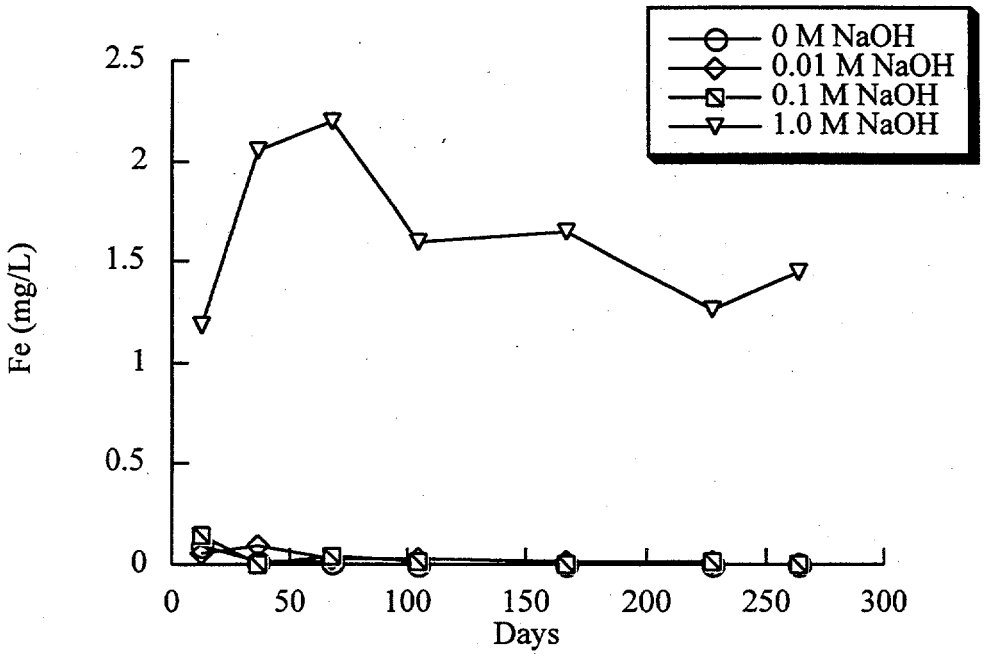

Figure 10. Effect of Influent NaOH Concentrations on Iron Concentrations in Composite Sediment Column Effluent (each data point represents the mean of two observations)

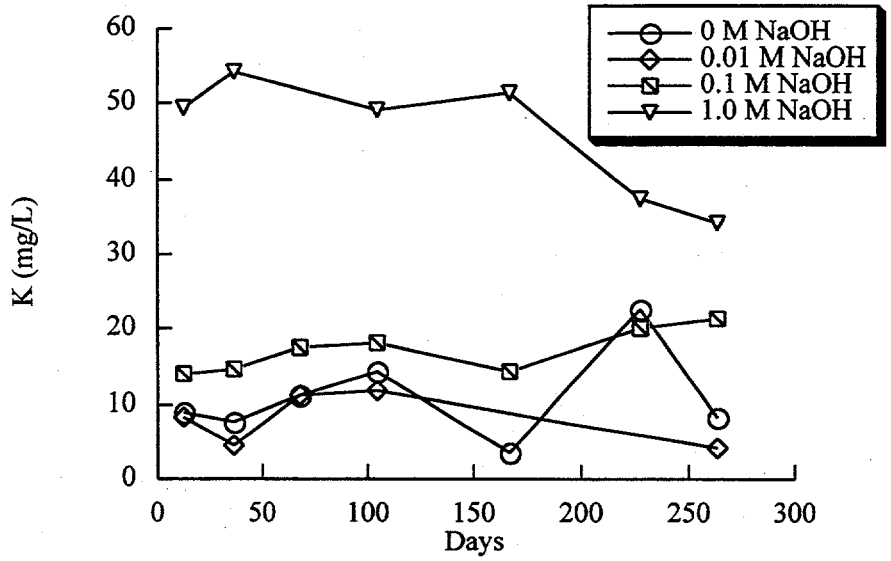

Figure 11. Effect of Influent NaOH Concentrations on Potassium Concentrations in Composite Sediment Column Effluent (each data point represents the mean of two observations)

Potassium exists in the composite sediments primarily in the structure of 2:1 minerals, such as mica-like minerals, and to an appreciably smaller extent on exchange sites of mineral surfaces. The K concentration of the composite sediment column effluent was presented in Figure 11. The K concentrations for the three lowest NaOH treatments remained essentially constant during the 264-day sample period. For the 1.0-M NaOH treatment, the K concentrations tended to decrease over time. Consistent with the Al and Fe concentration data, the K concentration data suggest appreciable dissolution of aluminosilicates in the 1.0-M NaOH treatment.

4.0 Conclusions

Column and batch experiments were conducted to evaluate the effect of varying concentrations of NaOH on sorptive, physical, and hydraulic properties of a quartz sand and a composite sediment from the Hanford Site. The NaOH solutions were used to simulate a simplified leachate from a low-activity glass waste form. Although the precise composition of the leachate for the waste-form glass is not known, it is known that the dominant cation will be sodium and the dominant anion will be hydroxide. The simulated leachate concentrations used in these experiments (0 to 1.0 M NaOH) represents an extended range of likely concentrations of sodium and hydroxide that will exist in the near field of the ILAW-DC. By using this simplified glass leachate, some potentially important chemical processes could not be evaluated. For example, the simplified glass leachate did not permit evaluation of the effects of certain electrolytes on the formation of some secondary minerals or their competition with radionuclides for sediment sorption sites. However, these studies provided an important first approximation of several chemical and physical processes that have not been studied, either at Hanford or elsewhere. In particular, there has not been any research conducted to evaluate the effect of glass waste-form leachate on the dissolution of the sediment or backfill. It is known that highly alkaline solutions can cause dissolution of silicates (such as quartz and amorphous silicates) and aluminosilicates (such as smectites, illites, and vermiculites). It is not known whether this dissolution will impact sorptive, physical, and hydraulic properties of the native sediments and backfill. In a simplified manner, it was expected that the smaller particles, which would include the amorphous silicates and the highly sorptive aluminosilicate clays, would be more likely to dissolve because they have the greatest surface area for the simulated leachate to react with. The dissolution of these minerals was expected to alter not only sorption properties but also the physical and hydraulic properties of the sediments/backfill. If the finer particles were to dissolve, then an increase in hydraulic conductivity would be expected. If the solid phase were to dissolve and then reprecipitate, it is expected that plugging of the porous media would occur.

A quartz sand was used to estimate the impact of the dissolution process on the hydraulic properties of material that may be placed around the burial site to create a capillary break that will hinder moisture migration into the waste glass. Some preliminary modeling of the near field indicated that diffusion may cause some of the waste-form leachate to migrate upward toward the capillary-break barrier (Mann et al. 1998). If this highly alkaline leachate were to cause dissolution of the barrier material, then the physical integrity of the barrier would be degraded and the functionality of the barrier (i.e., its ability to provide a physical barrier to water movement) would be compromised.

The second material used was a composite of archived Hanford Site sediment from three boreholes from the 200-East Area. This material was selected to simulate a backfill material that may be used to provide an inexpensive material to fill voids between the engineered materials and waste forms.

When the composite sediment was put in contact with the NaOH solutions, dissolution was evident based on the substantial increase in dissolved Si concentrations. Incremental increases in NaOH concentrations resulted in corresponding increases in Si solution concentrations. As much as 1,944 mg/L Si were measured in NaOH-treatment solutions, whereas only ~7 mg/L Si were measured in the 0-M NaOH treatment. A number of physical and hydraulic properties also changed as the NaOH concentrations were increased. These changes were especially dramatic in the dynamic flow experiments but were not as systematic in the batch experiments. In the sediment column experiments, as the influent NaOH concentrations were increased from 0 to 1.0 M, the hydraulic conductivity increased from 0.24 to 0.55 cm/min, the porosity increased from 0.34 to 0.44 cm^3/cm^3, and the bulk density decreased from 1.87 to 1.72 g/cm^3. All three changes are indicative of matrix dissolution.

The quartz sand dissolved appreciably less than the composite sediment dissolved. After 10 months, the Si concentration in the aqueous phase of the quartz sand batch experiment was 4 mg/L in the 0-M NaOH treatment and 189 mg/L in the 1.0-M NaOH treatment. The dissolution of the quartz sand had little measurable effect on the physical and hydrologic properties measured, though some change was evident in the column experiment. As the influent NaOH concentrations were increased from 0 to 1.0 M, the hydraulic conductivity increased from 8.70 to 10.15 cm/min, the porosity increased from 0.39 to 0.40 cm^3/cm^3, the bulk density increased from 1.60 to 1.67 g/cm^3, but there was no significant change in the particle-size distribution. These changes were quite moderate and, in some cases, were not statistically significant.

Moisture-retention measurements were made on the quartz sand and composite sediment. The moisture-retention measurements consistently showed that the 1.0-M NaOH-treated solids retained more water than the 0-M NaOH-treated solids. Because the other chemical, physical, and hydraulic measurements suggested that dissolution and not precipitation occurred in the high-NaOH treatments, the greater moisture retention of the high-NaOH treatments was attributed to a salt effect and not to the formation of small particles. Increases in NaOH concentrations, as well as most other hydrophilic solutes, can increase moisture retention by increasing capillary forces (water tension) and water adsorption to the sediments (by saturating the solid-phase surfaces with highly hydrated sodium ions).

The NaOH-treated composite sediment was used to measure Cs, Sr, and U K_d values. The purpose of these measurements was to determine whether the sorptive properties of NaOH-aged sediments were altered with respect to natural sediments. It was expected that the extent of radionuclide sorption would decrease because of the dissolution of smaller minerals or because of greater concentrations of competing Na ions present in the simulated leachates. Cs, Sr, and U were selected for the sorption experiments because they have unique geochemical properties (monovalent, divalent, and complexing cationic radionuclides, respectively) and are important dose contributors to the ILAW-PA. Additionally, Cs and Sr tend to adsorb well to sediments; therefore, it was expected that changes in the composite sediment's mineral composition would be easily observed as changes in the extent that these two radionuclides adsorbed.

There were a number of complications encountered in the sorption experiments. The U K_d measurements were not successful because of U(VI) measurement problems in the highly alkaline simulated glass leachate. The U(VI) measurements may be completed in fiscal year 1999, using a more-expensive analytical technique (ICP-MS). Additional problems arose in the sorption experiments, in that algae growth became evident after 10 months of contact time. Thus, Cs and Sr K_d values were obtained from sediments aged for 0, 1, and 2 months but not 12 months as initially planned. Finally, the sorption experiments for the 0-M NaOH treatment had a significant amount of Cs and Sr sorbed to the labware, as indicated by the filtration ratio being appreciably <1. This compromised interpretation of the data.

Some important results were obtained from the limited sorption data collected. The Cs K_d values decreased from ~3,000 to 1,000 mL/g as the NaOH concentrations increased from 0.01 to 1.0 M NaOH. The duration that the sediment was in contact with the NaOH treatments did not have any effect on Cs K_d values. Similarly, Sr K_d values decreased from ~1,300 to 300 mL/g as the NaOH concentrations increased from 0.01 to 1.0 M NaOH. There was no apparent trend in Sr K_d values with contact time. The lack of trend between the K_d values and contact time suggests that the cause for the decrease in K_d values with increased NaOH-concentration treatment was not the result of the dissolution of sediment particles but was caused by competition of the added Na.

In summary, the NaOH-concentration treatments caused two types of effects on the two solids studied. The first effect can be attributed to dissolution of some of the composite sediment. The measurable increase in porosity and decrease in bulk density observed for the composite sediment suggest that dissolution occurred. Together, these changes could have been responsible for the slight increase in hydraulic conductivity. The second effect can be attributed to a change in the aqueous phase of the system (i.e., the added NaOH increased the concentration of the Na^+ and OH^- ions). This salt effect manifested itself in two or three distinct ways. First, the salt effect appears to be responsible for the significant decrease in Cs and Sr K_d values. The added Na competed with Cs and Sr for sorption sites. The decrease in K_d values was instantaneous, occurring with a contact time of 0 month. As the contact time increased to 2 months, no change in K_d values was observed, even though physical changes in the sediment had been measured during this period. The second salt effect increased moisture retention. The increased amount of moisture retained by the NaOH-treated composite sediment did not change with contact time. If dissolution-induced changes were the cause of changes in moisture retention, more time dependence would have been seen. Finally, the increase in salt concentration may have induced an increase in fluidity, thereby increasing hydraulic conductivity.

These experiments were conducted over a limited contact time with respect to the 10,000- to 100,000-year scenarios being described by the ILAW-PA. Yet, it is clear from these experiments that the chemical composition of the waste-glass leachate is likely to have significant effects on hydrology and radionuclide geochemistry in the near-field environment. These effects may make the ILAW-DC more or less suitable for waste immobilization than would be estimated based on experiments conducted with "unaged" materials. The glass waste-form leachate may make the near field less suitable for waste immobilization by increasing the hydraulic conductivity via particle dissolution and/or increased fluidity and by decreasing the sorption capacity of the sediments via the salt effect. However, it could also make the system more suitable for waste immobilization by increasing the moisture retention via the salt effect, increasing sorption (e.g., Tc and Se; Kaplan et al. 1998d), or inducing precipitation (e.g., U[VI]; Kaplan

et al. 1996). Additional research will be conducted in fiscal year 1999 to identify more thoroughly the mechanisms of the processes described herein. Future research will apply more direct measurement of these processes (e.g., using an x-ray tomography unit) and will be conducted using more-complex, simulated glass leachate than was used in these experiments. Particular attention will be directed at quantifying the reaction rates of the mineral dissolution and defining the solid-phase composition of a typical Hanford Site backfill sediment after extended exposure to the glass waste-form leachate. This future research, together with the data presented in this report, will provide important guidance for the selection of near-field hydraulic and geochemical data for the ILAW-PA.

5.0 References

Ames LL, and D Rai. 1978. *Radionuclide interactions with soil and rock media. Volume 1: Processes influencing radionuclide mobility and retention, element chemistry and geochemistry, conclusions, and evaluation.* PBS292460, Office of Radiation Programs, U.S. Environmental Protection Agency, Las Vegas, Nevada.

Ames LL, and RJ Serne. 1991. *Compilation of data to estimate groundwater migration potential for constituents in active liquid discharges at the Hanford Site.* PNL-7660, Pacific Northwest Laboratory, Richland, Washington.

Anderson MS. 1926. *Properties of soil colloidal material.* Bulletin Number 1452, U.S. Department of Agriculture, Beltsville, Maryland.

Brina R, and AG Miller. 1992. "Direct detection of trace levels of uranium by laser-induced kinetic phosphorimetry." *Analytical Chemistry* 64:1413-1417.

Dress LR, LP Wilding, NE Smeck, and AL Senkayi. 1989. "Silica in soils: Quartz and disordered silica polymorphs." In *Minerals in soil environments*, JB Dixon and SB Week (eds.), second edition, pp. 913-974, Soil Science Society of America, Madison, Wisconsin.

Freeze FA, and JA Cherry. 1979. *Groundwater.* Prentice Hall, Englewood Cliffs, New Jersey.

Gardner WR. 1968. "Availability and measurement of soil water." In *Water deficits and plant growth*, WR Garder (ed.), Volume 1, pp. 107-135, Academic Press, New York.

Hillel D. 1980. *Fundamentals of soil physics.* Academic Press, New York.

Janert H. 1934. "The application of heat of wetting measurements to soil research problems." *Journal of Agricultural Science* 24:136-145.

Kaplan DI, RJ Serne, AT Owen, J Conca, TW Wietsma, and TL Gervais. 1996. *Radionuclide adsorption distribution coefficients measured in Hanford sediments for the low-level waste performance assessment project.* PNNL-11385, Pacific Northwest National Laboratory, Richland, Washington.

Kaplan DI, KM Krupka, RJ Serne, SV Mattigod, and G Whelan. 1998a. "Selection of distribution coefficients for contaminant fate and transport calculations." In *1997 International Containment Technology Conference and Exhibition,* pp. 954-960, St. Petersburg, Florida, Florida State University Press, Tallahassee, Florida.

Kaplan DI, T Gervais, and KM Krupka. 1998b. "Coprecipitation of uranium in high pH and ionic strength environments." *Radiochimica Acta* 80(4):201-212.

Kaplan DI, KE Parker, and RD Orr. 1998c. *Effects of high-pH and high-ionic-strength groundwater on iodide, pertechnetate, and selenate sorption to Hanford sediments: Final report for subtask 3a.* PNNL-11964, Pacific Northwest National Laboratory, Richland, Washington.

Kaplan DI, KE Parker, and IV Kutynakov. 1998d. *Radionuclide distribution coefficients for sediments collected from borehole 299-E17-21: Final report for subtask 1a.* PNNL-11966, Pacific Northwest National Laboratory, Richland, Washington.

Mann FM, RJ Puigh, II, PD Rittmann, NW Kline, JA Voogd, Y Chen, CR Eiholzer, CT Kincaid, BP McGrail, AH Lu, GF Williamson, NR Brown, and PE LaMont. 1998. *Hanford immobilized low-activity tank waste performance assessment.* DOE/RL-97-69, Rev. 0, U.S. Department of Energy, Richland Operations Office, Richland, Washington.

Pacific Northwest Laboratory (PNL). 1988. *Procedures for ground-water investigations.* PNL-MA-567, Richland, Washington.

Pacific Northwest Laboratory (PNL). 1989. *Analytical chemistry laboratory (ACL) procedures compendium.* PNL-MA-599, Richland, Washington.

Parker KE. 1997. *Evaluation of the equilibrium sorption constant, K_d for sediment samples containing gravel.* Masters Thesis, Washington State University, Pullman, Washington.

Relyea JF, RJ Serne, and D Rai. 1980. *Methods for determining radionuclide retardation factors: Status report.* PNL-3349, Pacific Northwest Laboratory, Richland, Washington.

Ribbe RH. 1980. *Orthosilicates.* Volume 5, Book Crafters, Inc., Chelsea Michigan.

Sposito G. 1989. *The chemistry of soils.* Oxford University Press, New York.

Weast RC. 1988. *CRC handbook of chemistry and physics.* 69th edition, CRC Press, Inc., Boca Raton, Florida.

Appendix

Background Information and General Results

Table A.1. Borehole Samples Used to Make the Hanford Site Composite Sediment (to convert feet to meters, multiply by 0.3048)

Well	Depth (ft)	Wt. Tot. (kg)	Wt. Sample (kg)	Jar Label				Comments
Bucket #1, bucket tare = 0.774 kg								
299-E25-12	10	1.529	0.755	299-E25-12	11/19/60	10'		Mostly silt
	15	2.240	0.711	299-E25-12	11/19/60	15'		Mostly silt
	20	2.912	0.672	299-E25-12	11/19/60	20'		Mostly silt
	25	3.584	0.672	299-E25-12	11/19/60	25'		Mostly silt
	30	4.164	0.580	299-E25-12	11/19/60	30'		Sand
	35	4.649	0.485	299-E25-12	11/29/60	35'		Sand
	40	5.221	0.572	299-E25-12	11/21/60	40'		Sand
	45	5.744	0.523	299-E25-12	11/21/60	45'		Sand
299-E25-27	10	6.423	0.679	E25-27	4/10/85	10-15'	Core Barrel	Sand/some gravel
	10	7.216	0.793	E25-27	4/10/85	10-15'	Core Barrel	Sand/some gravel
	15	7.908	0.692	E25-27	4/10/85	15-20'	Core Barrel	Sand
	15	8.634	0.726	E25-27	4/10/85	15-20'	Core Barrel	Sand
	20	9.314	0.680	E25-27	4/11/85	20-25'	Core Barrel	Sand/some gravel
	20	10.010	0.696	E25-27	4/11/85	20-25'	Core Barrel	Sand
	25	10.646	0.636	E25-27	4/11/85	25-30'	Core Barrel	Sand
	25	11.321	0.675	E25-27	4/11/85	25-30'	Core Barrel	Sand
	30	12.001	0.680	E25-27	4/11/85	30-35'	Core Barrel	Sand
	30	12.647	0.646	E25-27	4/11/85	30-35'	Core Barrel	Sand
	35	13.304	0.657	E25-27	4/11/85	35-40'	Core Barrel	Sand
	35	13.928	0.624	E25-27	4/11/85	35-40'	Core Barrel	Sand
	40	14.606	0.678	E25-27	4/11/85	40-45'	Core Barrel	Sand
	40	15.285	0.679	E25-27	4/11/85	40-45'	Core Barrel	Sand
	45	15.921	0.636	E25-27	4/11/85	45-50'	Core Barrel	Sand
	45	16.559	0.638	E25-27	4/11/85	45-50'	Core Barrel	Sand

Table A.1. (contd)

Well	Depth (ft)	Wt. Tot. (kg)	Wt. Sample (kg)	Jar Label				Comments
299-E25-33	10	17.270	0.711	299-E25-33	11/12/87	10'	Core Barrel	Coarse sand
	15	17.797	0.527	299-E25-33	11/12/87	15'	Core Barrel	Fine sand/silt
	20	18.417	0.620	299-E25-33	11/12/87	20'	Core Barrel	Silt
	25	19.089	0.672	299-E25-33	11/12/87	25'	Core Barrel	Sand/gravel
	30	19.720	0.631	299-E25-33	11/16/87	30'	Core Barrel	Sand
	35	20.343	0.623	299-E25-33	11/16/87	35'	Core Barrel	Sand
Total sample weight for bucket #1 = 19.569 kg								
Bucket #2, bucket tare = 0.762 kg								
299-E25-33	40	1.373	0.611	299-E25-33	11/16/87	40'	Core Barrel	Sand
	45	1.996	0.623	299-E25-33	11/17/87	45'	Core Barrel	Sand
299-E25-26	10	2.746	0.750	E25-26	3/1/85	10'	Core Barrel	Mostly silt
	15	3.339	0.593	E25-26	3/1/85	15'	Core Barrel	Mostly silt
	30	3.893	0.554	E25-26	3/1/85	30-35'	Core Barrel	Sand
	35	4.600	0.707	E25-26	3/1/85	35-40'	Core Barrel	Sand
	40	5.229	0.629	E25-26	3/1/85	40-45'	Core Barrel	Sand
299-E25-28	10	5.757	0.528	299-E25-28	2/25/86	10-15'	Core Barrel	Fine sand
	15	6.458	0.701	299-E25-28	2/25/86	15-20'	Core Barrel	Sand
	20	7.092	0.634	299-E25-28	2/25/86	20-25'	Core Barrel	Sand/gravel
	25	7.634	0.542	299-E25-28	2/25/86	25-30'	Core Barrel	Sand
	30	8.144	0.510	299-E25-28	2/25/86	30-35'	Core Barrel	Sand
	35	8.693	0.549	299-E25-28	2/25/86	35-40'	Core Barrel	Sand
	40	9.288	0.595	299-E25-28	2/25/86	40-45'	Core Barrel	Sand
299-E24-6	15	9.858	0.570	216-A-9 #4	6/28/56	15'	E24-6	Coarse sand
	20	10.469	0.611	216-A-9 #4	6/28/56	20'	E24-6	Silt/sand/gravel
	25	10.980	0.511	216-A-9 #4	6/28/56	25'	E24-6	Coarse sand

Table A.1. (contd)

Well	Depth (ft)	Wt. Tot. (kg)	Wt. Sample (kg)	Jar Label				Comments
299-E24-6 (contd)	30	11.516	0.536	216-A-9 #4	6/28/56	30'	E24-6	Coarse sand
	35	12.121	0.605	216-A-9 #4	6/28/56	35'	E24-6	Coarse sand/gravel
	40	12.721	0.600	216-A-9 #4	6/29/56	40'	E24-6	Coarse sand/gravel
	45	13.308	0.587	216-A-9 #4	6/29/56	45'	E24-6	Coarse sand/gravel
	50	13.851	0.543	216-A-9 #4	6/29/56	50'	E24-6	Coarse sand
299-E25-1	30	14.153	0.302	Well 241-A-1	2/4/55	30'	E25-1	Silt/gravel
	35	14.540	0.387	Well 241-A-1	2/4/55	35'	E25-1	Silt/gravel
	40	14.823	0.283	Well 241-A-1	2/4/55	40'	E25-1	Silt
	45	15.260	0.437	Well 241-A-1	2/4/55	45'	E25-1	Silt/gravel
	50	15.636	0.376	Well 241-A-1	2/4/55	50'	E25-1	Silt/gravel
299-E25-2	15	16.236	0.600	216-A-1 #6	2/3/54	15'	E25-2	Silt
	20	17.065	0.829	216-A-1 #6	2/4/54	20'	E25-2	Silt/sand
	25	17.765	0.700	216-A-1 #6	2/4/54	25'	E25-2	Silt/sand
	30	18.497	0.732	216-A-1 #6	2/4/54	30'	E25-2	Sand
Total sample weight for bucket #2 = 17.735 kg								
Bucket # 3, bucket tare = 0.758 kg								
299-E25-2	35	1.520	0.762	216-A-1 #6	2/4/54	35'	E25-2	Sand
	40	2.140	0.620	216-A-1 #6	2/4/54	40'	E25-2	Sand
	45	2.854	0.714	216-A-1 #6	2/4/54	45'	E25-2	Sand
	50	3.531	0.677	216-A-1 #6	2/4/54	50'	E25-2	Sand
299-E25-43	10	4.077	0.546	299-E25-43	6/12/91	10'	Drive barrel	Sand
	15	4.595	0.518	299-E25-43	6/13/91	15'	Drive barrel	Sand
	20	5.117	0.522	299-E25-43	6/13/91	20'	Drive barrel	Sand
	25	5.633	0.516	299-E25-43	6/13/91	25'	Drive barrel	Sand
	30	6.195	0.562	299-E25-43	6/13/91	30'	Drive barrel	Sand

Table A.1. (contd)

Well	Depth (ft)	Wt. Tot. (kg)	Wt. Sample (kg)	Jar Label				Comments
299-E26-12	10	6.750	0.555	299-E26-12	6/5/91	10'	Core barrel	Sand
	15	7.388	0.638	299-E26-12	6/7/91	15'	Core barrel	Sand
	20	7.803	0.415	299-E26-12	6/7/91	20'	Core barrel	Sand/silt
	25	8.382	0.579	299-E26-12	6/7/91	25'	Core barrel	Sand/silt
	30	8.920	0.538	299-E26-12	6/7/91	30'	Core barrel	Sand/1 white rock
299-E26-13	10	9.615	0.695	299-E26-13	6/4/91	10'	Drive barrel	Sand/silt
	15	10.160	0.545	299-E26-13	6/4/91	15'	Drive barrel	Sand/silt
	20	10.834	0.674	299-E26-13	6/4/91	20'	Drive barrel	Sand/silt
299-E25-25	10	11.553	0.719	E25-25	3/11/85	10-15'	Core barrel	Sand/silt
	15	12.219	0.666	E25-25	3/11/85	15-20'	Core barrel	Sand/silt
	20	12.940	0.721	E25-25	3/11/85	20-25'	Core barrel	Sand
	25	13.535	0.595	E25-25	3/11/85	25-30'	Core barrel	Sand
	30	14.155	0.620	E25-25	3/12/85	30-35'	Core barrel	Sand
	35	14.764	0.609	E25-25	3/12/85	35-40'	Core barrel	Sand
	40	15.318	0.554	E25-25	3/12/85	40-45'	Core barrel	Sand
Total sample weight for bucket #3 = 14.560 kg								
Total sample weight = 51.864 kg								

Table A.2. Moisture-Retention Data

Quartz Sand Batch Experiment

0M NaOH/10mo		1M NaOH/10mo		0M NaOH/1mo		1M NaOH/1mo	
Pressure (bar)	Moisture (%)	Pressure (bar)	Moisture (%)	Pressure (bar)	Moisture (%)	Pressure (bar)	Moisture (%)
0.01	0.38	0.01	0.38	0.01	0.37	0.01	0.38
0.55	0.0264	0.55	0.0383	0.55	0.0204	0.55	0.0196
1	0.0145	1	0.0281	1	0.0085	1	0.0145
2.02	0.0094	2.02	0.0145	2.02	0.0068	2.02	0.0136
4	0.0051	4	0.0136	4	0.0060	4	0.0136
1,221.57	0.0026	1,219.86	0.0026	1,194.27	0.0024	1,205.35	0.0044

Hanford Site Composite Sediment Batch Experiment

0M NaOH/10mo		1M NaOH/10mo		0M NaOH/1mo		1M NaOH/1mo	
Pressure (bar)	Moisture (%)	Pressure (bar)	Moisture (%)	Pressure (bar)	Moisture (%)	Pressure (bar)	Moisture (%)
0.01	0.29	0.01	0.33	0.01	0.28	0.01	0.33
0.55	0.1098	0.55	0.1021	0.55	0.0928	0.55	0.097872
1	0.0885	1	0.0928	1	0.0791	1	0.090213
2.02	0.08	2.02	0.0911	2.02	0.0681	2.02	0.0860
4	0.0749	4	0.0860	4	0.0630	4	0.08
1,065.84	0.0228	1,064.06	0.0183	1,073.04	0.0217	1,125.83	0.0158

Column Experiment

Sand/0M/10 mo		Sand/1M/10 mo		Sed/0M/10 mo		Sed/1M/10 mo	
Pressure (bar)	Moisture (%)	Pressure (bar)	Moisture (%)	Pressure (bar)	Moisture (%)	Pressure (bar)	Moisture (%)
0.01	0.39	0.01	0.4	0.01	0.34	0.01	0.32
0.55	0.0340	0.55	0.0204	0.55	0.1013	0.55	0.0894
1	0.0187	1	0.0119	1	0.0817	1	0.0723
2.02	0.0077	2.02	0.0085	2.02	0.0809	2.02	0.0655
4	0.0068	4	0.0060	4	0.0740	4	0.0570
1,246.85	0.0025	1,277.86	0.0024	1,061.43	0.0239	1,068.47	0.0223

Untreated Sand and Sediment Samples

Quartz Sand		Composite Sediment	
Pressure (bar)	Moisture (%)	Pressure (bar)	Moisture (%)
0.01	0.39	0.01	0.32
0.55	0.0145	0.55	0.0894
1	0.0094	1	0.0723
2.02	0.0077	2.02	0.0655
4	0.0060	4	0.0570
1,232.05	0.0027	1,068.47	0.0223

Table A.3. Aqueous Chemical Composition of Batch Experiments

Contact Time (month)	Solid Phase	NaOH (M)	Al (mg/L)	Fe (mg/L)	Si (mg/L)	B (mg/L)	K (mg/L)
1	Quartz sand	0.00	0.07	0.00	6.99	2.00	1.83
		0.01	2.44	0.04	27.52	2.84	0.00
		0.10	7.18	0.00	44.81	3.12	0.00
		1.00	25.21	0.83	127.12	5.87	0.00
	Composite sediment	0.00	0.25	0.02	26.89	2.73	0.00
		0.01	0.39	0.48	39.99	1.91	3.59
		0.10	7.18	0.01	323.25	1.21	11.90
		1.00	125.45	0.82	1,282.30	3.73	76.86
2	Quartz sand	0.00	0.23	0.02	8.60	2.36	21.80
		0.01	2.85	0.11	28.41	2.29	21.58
		0.10	8.25	0.05	50.56	3.01	24.75
		1.00	32.40	1.28	151.20	4.82	19.60
	Composite sediment	0.00	0.07	0.00	23.87	2.15	8.96
		0.01	0.47	0.54	38.42	1.98	6.15
		0.10	5.99	0.05	356.23	1.73	10.34
		1.00	135.29	0.71	1,663.90	3.69	81.94
10	Quartz sand	0.00	0.08	0.00	3.55	0.00	6.57
		0.01	2.72	0.00	26.52	0.00	5.76
		0.10	9.64	0.00	53.42	0.00	10.43
		1.00	53.87	0.00	188.91	0.01	17.96
	Composite sediment	0.00	0.02	0.00	12.82	0.00	4.09
		0.01	0.47	0.71	18.32	0.00	3.11
		0.10	1.67	0.00	368.67	0.00	7.07
		1.00	100.66	0.21	1,944.50	0.10	95.98

Table A.4. Column Effluent Chemical Composition (mg/L)

Quartz Sand 0 M NaOH Treatment							
	13 Days	36 Days	68 Days	104 Days	167 Days	228 Days	264 Days
Al	0.71	0.48	0.39	0.00	0.00	0.15	0.01
B	6.05	4.20	4.86	8.85	6.53	3.14	0.24
Ba	0.00	0.02	0.02	0.03	0.03	0.00	0.00
Ca	1.18	0.01	0.00	0.09	0.00	0.07	0.00
Fe	0.00	0.05	0.00	0.00	0.00	0.00	0.00
K	4.61	6.97	8.83	1.14	2.40	5.60	4.31
Na	181.43	249.30	126.67	10.08	8.31	24.37	1.13
Si	15.31	14.30	11.11	14.68	12.65	6.10	0.00

Quartz Sand 0.1 M NaOH Treatment							
	13 Days	36 Days	68 Days	104 Days	167 Days	228 Days	264 Days
Al	4.36	4.34	3.90	2.40	4.34	2.92	2.56
B	5.38	6.06	6.85	7.12	14.84	5.38	0.06
Ba	0.02	0.03	0.00	0.05	0.09	0.03	0.00
Ca	1.26	1.26	0.30	0.09	0.13	0.28	0.00
Fe	0.10	0.09	0.02	0.01	0.05	0.04	0.00
K	8.51	9.47	7.82	4.25	0.00	4.28	8.32
Na	2,672	3,144	2,181	1,848	2,486	2,168	1,705
Si	47.55	48.32	49.79	50.30	90.97	44.15	10.88

Composite Sediment 0 M NaOH Treatment							
Days	13 Days	36 Days	68 Days	104 Days	167 Days	228 Days	264 Days
Al	0.00	0.02	0.20	0.18	0.09	0.07	0.05
B	5.56	3.21	4.42	6.72	4.24	2.12	0.07
Ba	0.01	0.05	0.00	0.00	0.04	0.06	0.02
Ca	5.20	4.98	3.94	2.89	3.95	3.12	1.92
Fe	0.10	0.02	0.01	0.00	0.00	0.00	0.00
K	8.95	7.64	11.31	14.45	3.49	1.40	3.22
Na	144.79	187.74	113.98	26.93	5.54	22.80	8.26
Si	31.66	23.35	21.97	24.72	18.18	10.86	7.17

Composite Sediment 0.1 M NaOH Treatment							
Days	13 Days	36 Days	68 Days	104 Days	167 Days	228 Days	264 Days
Al	9.20	27.81	24.05	23.53	21.09	20.58	19.35
B	1.99	3.53	3.91	1.84	4.36	3.08	0.09
Ba	0.00	0.01	0.01	0.00	0.01	0.08	0.03
Ca	2.79	0.30	0.75	0.16	0.43	0.76	0.44
Fe	0.15	0.00	0.04	0.01	0.00	0.01	0.00
K	13.92	14.66	17.72	18.05	14.44	20.10	21.51
Na	2,017.70	2,266.1	2,368.20	1,686.60	2,188.20	2,143.60	1,702.50
Si	292.06	217.23	183.65	149.20	162.92	136.30	117.14

Table A.4. (contd)

Quartz Sand 0.01 M NaOH Treatment							
	13 Days	36 Days	68 Days	104 Days	167 Days	228 Days	264 Days
Al	2.31	1.29	0.80	0.12	0.27	0.80	0.75
B	4.26	3.72	2.75	8.28	7.99	2.99	0.09
Ba	0.00	0.02	0.00	0.02	0.03	0.04	0.00
Ca	0.80	0.56	0.60	0.07	0.00	0.00	0.00
Fe	0.00	0.08	0.03	0.06	0.10	0.03	0.05
K	1.81	8.57	7.90	0.00	1.45	3.10	4.53
Na	365.58	693.33	255.24	227.68	263.13	257.49	187.46
Si	26.75	20.87	10.78	25.38	25.88	13.00	4.24

Quartz Sand 1.0 M NaOH Treatment							
	13 Days	36 Days	68 Days	104 Days	167 Days	228 Days	264 Days
Al	11.35	10.54	9.06	10.60	9.83	6.44	4.91
B	7.70	10.57	10.09	20.19	14.94	11.04	0.15
Ba	0.08	0.07	0.07	0.08	0.15	0.08	0.05
Ca	1.27	0.30	0.24	0.50	0.29	0.50	0.00
Fe	1.07	0.83	0.50	0.34	0.30	0.29	0.23
K	8.12	6.78	11.00	9.06	8.81	7.00	9.15
Na	18,176	18,176	14,261	14,966	18,215	16,261	12,210
Si	103.22	111.69	101.93	201.80	147.44	112.20	17.70

Composite Sediment 0.01 M NaOH Treatment							
	13 Days	36 Days	68 Days	104 Days	167 Days	228 Days	264 Days
Al	0.09	1.78	3.62	2.89	4.50	4.46	7.02
B	6.05	3.94	3.70	6.93	4.44	1.79	0.01
Ba	0.03	0.03	0.03	0.00	0.05	0.10	0.00
Ca	4.12	1.21	0.61	0.30	0.53	1.16	0.52
Fe	0.06	0.09	0.03	0.03	0.01	0.01	0.00
K	8.22	4.55	11.23	11.79	--[a]	--[a]	5.01
Na	129.32	393.39	324.39	213.25	228.86	245.10	201.01
Si	44.92	82.45	74.67	57.65	58.84	50.40	46.82

Composite Sediment 1.0 M NaOH Treatment							
	13 Days	36 Days	68 Days	104 Days	167 Days	228 Days	264 Days
Al	103.54	84.89	59.87	54.67	65.51	44.14	39.282
B	10.19	6.23	7.14	9.36	10.90	6.47	0.21
Ba	0.01	0.03	0.01	0.00	0.05	0.04	0.00
Ca	1.58	0.45	0.00	0.25	0.46	1.02	0.86
Fe	1.18	2.05	2.19	1.59	1.65	1.27	1.45
K	49.62	54.31	--[a]	49.25	51.27	37.27	34.06
Na	18,176	14,261	14,261	14,509	17,222	16,095	12,571
Si	771.37	599.05	471.14	416.73	514.64	328.90	247.80

(a) ICP instrument malfunction for K channel.

Distribution

No. of Copies

OFFSITE

3 D. I. Kaplan
Westinghouse Savannah River Company
773-A Room B121
Aiken, SC 29802

ONSITE

5 **DOE Richland Operations Office**

N. R. Brown	A0-12
M. J. Furman	H0-12
P. E. LaMont	H0-12
J. A. Poppiti	S7-54
K. M. Thompson	H0-12

Fluor Daniel Hanford, Inc.

J. D. Williams	S7-40

5 **Fluor Daniel Northwest, Inc.**

F. M. Mann (4)	B4-43
R. Khaleel	B4-43

No. of Copies

4 **Lockheed Martin Hanford Corporation**

E. A. Fredenburg	R1-04
D. A. Myers	R1-04
J. A. Voogd	S4-45
R. W. Root	R2-53

Waste Management Federal Services, Inc.

M. I. Wood	H6-06

30 **Pacific Northwest National Laboratory**

M. J. Fayer	K9-33
G. W. Gee	K9-33
V. G. Johnson	K6-96
C. T. Kincaid	K9-33
I. V. Kutynakov	K6-81
S. V. Mattigod	K6-81
B. P. McGrail	K6-81
K. E. Parker (2)	K6-81
S. P. Reidel	K6-81
J. C. Ritter (2)	K9-33
R. J. Serne (10)	K6-81
R. M. Smith	K6-96
Information Release Office (7)	K1-06